NATIONAL AERONAUTICS AND SPACE ADMINISTRATION

Technical Report 32-1478

A Frequency Domain Solution for the Linear Attitude-Control Problem of Spacecraft With Flexible Appendages

M. R. Trubert

JET PROPULSION LABORATORY
CALIFORNIA INSTITUTE OF TECHNOLOGY
PASADENA, CALIFORNIA

November 15, 1970

NATIONAL AERONAUTICS AND SPACE ADMINISTRATION

Technical Report 32-1478

A Frequency Domain Solution for the Linear Attitude-Control Problem of Spacecraft With Flexible Appendages

M. R. Trubert

JET PROPULSION LABORATORY
CALIFORNIA INSTITUTE OF TECHNOLOGY
PASADENA, CALIFORNIA

November 15, 1970

Prepared Under Contract No. NAS 7-100
National Aeronautics and Space Administration

Preface

The work described in this report was performed by the Engineering Mechanics Division of the Jet Propulsion Laboratory.

Acknowledgment

This study was done in collaboration with the Spacecraft Control Section of JPL. Gerald Fleischer furnished the control parameters used in the control loop. The author is indebted to John Garba of the Applied Mechanics Section for his invaluable contribution to the preparation of the numerical solution of the problem. His numerous suggestions have helped to clarify the whole problem. The actual programming was done by Mrs. Carolyn Level.

Contents

Table

Figures

Contents (contd)

Figures (contd)

Abstract

The three-dimensional linear interaction problem between attitude control of spacecraft and the flexibility of spacecraft is solved in the frequency domain by using the concept of Fourier transform. The transfer-function matrix of the system formed by the linear structure and the linear control circuit is determined from the modal characteristics of the structure, using the modal combination concept and the electrical characteristics of the control loop. A large number of elastic modes can be used for the structure. Time histories are obtained by inverse Fourier transformation. The three angles of the attitude of the spacecraft with respect to an inertial frame of reference are computed for any disturbance torques applied about the three axes of the spacecraft. A stability study is made by direct inspection of the responses to unit impulse for the three attitude angles or, alternatively, by the display of a determinant. A computer program has been written to compute all of the necessary transfer functions, and the fast Fourier transform algorithm has been used to compute Fourier transforms. The program is used on a teletype terminal.

A Frequency Domain Solution for the Linear Attitude-Control Problem of Spacecraft With Flexible Appendages

I. Introduction

The anticipated advent of spacecraft with large, flexible appendages, such as long solar panels or large antennas, introduces vibrational structural modes that fall in the frequency range of the attitude-control system. Consequently, a coupling exists between structural flexibility and the attitude-control system and imposes constraints on the study of the stability of the system. This problem has been reviewed and studied at length (Ref. 1).

A nontraditional frequency-domain/Fourier-transform approach is proposed in this report. Small motion is assumed to linearize the equations. The open-loop transfer function (frequency response) of the flexible spacecraft, relating the attitude angles to the control parameters, is computed numerically in terms of discrete real frequencies over the frequency range of interest. The problem is then specialized to attitude control by control jets, the transfer function of the control loop is introduced, and the transfer function of the closed-loop system relating attitude angles to a disturbance is computed numerically. The response to any external transient disturbance torque can be computed first in the frequency domain, then in the time domain, by inverse Fourier transformation. The stability of the system can be studied by the concept of the response to the unit impulse. Use of real frequency ω associated with the Fourier transform technique permits a numerical computation of the time history of the response to the unit impulse by inverse Fourier transformation, giving a stability criterion by direct inspection.

The Fourier transform technique is in contrast with the more traditional Laplace transform technique, which is usually limited to algebraic computation in terms of a complex argument s. The proposed technique has the further advantage over the Laplace method of permitting the use of a large number of elastic modes without any computational difficulties.

II. Technical Discussion

Let it be assumed that the spacecraft is composed of a rigid bus and flexible appendages, such as solar panels or antennas attached to the bus (Fig. 1). Small motion will be assumed to linearize the equations. The frequency-domain approach will be used when convenient.

A. Equations of Motion of One Appendage

The appendage is attached to the bus at a number of points that have no relative displacement because the bus is assumed to be rigid. The attachment points are referred to as the base of the appendage. It is then natural and convenient to introduce the flexibility of the appendage in its deflection with respect to those attachment points. The corresponding modes of vibration will be called *cantilever modes* (i.e., modes for which the base is fixed, as shown in Fig. 2).

With reference to Fig. 1, $Ax_1x_2x_3$ is a system of coordinates of origin A fixed with respect to the bus to describe the motion of the appendage relative to the bus. This system will be referred to as the x system of coordinates. Let it be assumed that p forces $\mathscr{F}^1, \mathscr{F}^2, \cdots, \mathscr{F}^p$ are applied to the appendage at points $P_1, P_2, \cdots, P_p$ (see Fig. 2). If small motion and proportional damping are assumed (Ref. 2), the equations of motion of the appendage, expressed in terms of the cantilevered n normal modes, are

$$m_j(\ddot{q}_j + 2\omega_j\xi_j\dot{q}_j + \omega_j^2 q_j) = \sum_{k=1}^{3p} \phi_{jk}\mathscr{F}_k \qquad j = 1, 2, \cdots, n \qquad (1)$$

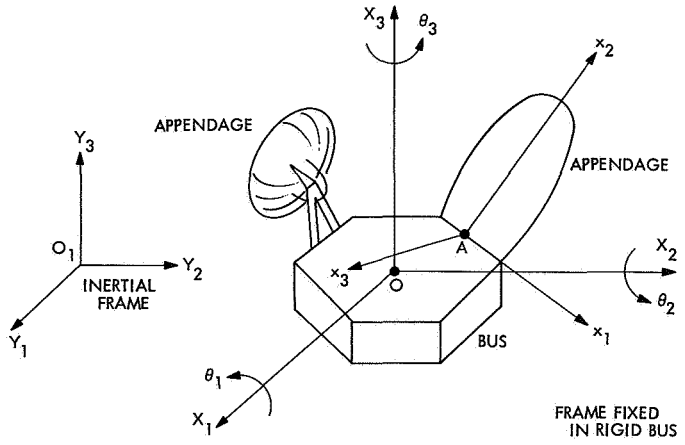

Fig. 1. Sketch of spacecraft bus and appendages

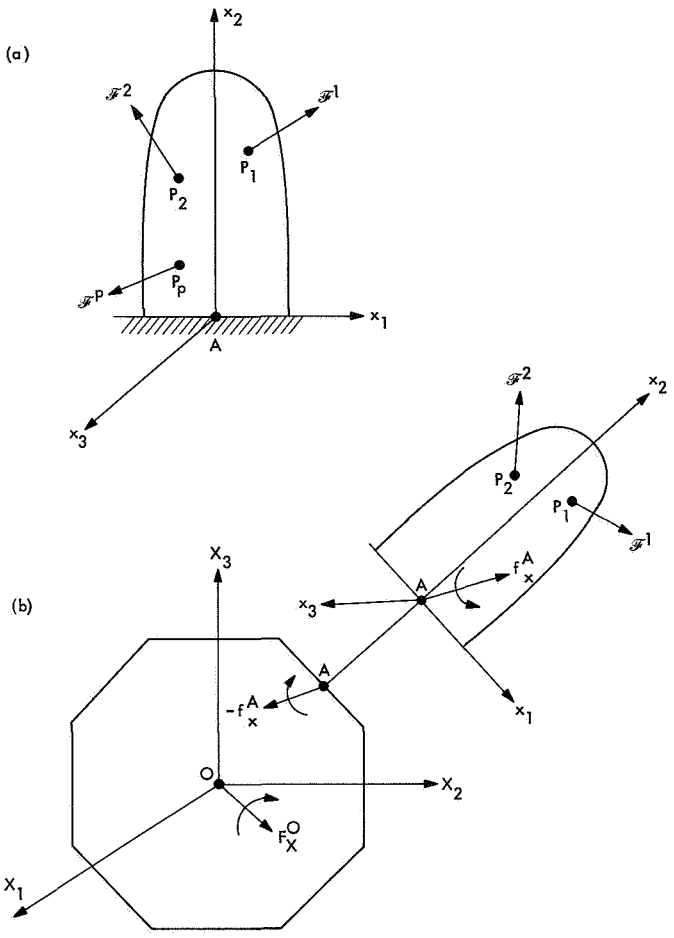

Fig. 2. Cantilever modes: (a) cantilevered appendage; (b) free body diagram for appendage and bus

where

m_j = generalized masses

ω_j = natural frequencies

ξ_j = modal dampings

q_j = generalized displacements

$\mathscr{F}_k (k = 1, 2, \cdots, 3p)$ = all components of p forces at $P_1, P_2, \cdots, P_p$

ϕ_{jk} = corresponding mode shapes at those points

Equation(s) (1) can be written in matrix form as follows:

$$\mathbf{M}_{ee}\ddot{\mathbf{q}} + \mathbf{C}_{ee}\dot{\mathbf{q}} + \mathbf{K}_{ee}\mathbf{q} = \boldsymbol{\phi}_e^T \mathscr{F} \qquad (2)$$

where

$\mathbf{M}_{ee} = [\ m_j\ ] = n \times n$ generalized mass matrix

$\mathbf{C}_{ee} = [\ 2\omega_j \xi_j m_j\ ] = n \times n$ generalized damping matrix

$\mathbf{K}_{ee} = [\ \omega_j^2 m_j\ ] = n \times n$ generalized stiffness matrix

$\mathbf{q} = \{q_j\}$ = column of generalized displacements

$\mathscr{F} = \{\mathscr{F}_k\}$ = column of components of forces applied at points $P_1, P_2, \cdots, P_p$

$\boldsymbol{\phi}_e = [\phi_{kj}]$ = $3p \times n$ matrix of elastic mode shapes at $P_1, P_2, \cdots, P_p$

The equations of motion of the appendage with respect to an inertial frame $O_1Y_1Y_2Y_3$ of reference can be obtained from Eq. (1) in the standard manner by "freeing" the system of Eq. (2) (Ref. 3). Small rotation of the base of the appendage is assumed. Because the base is attached to the bus, reaction forces and moments exist on the base and must be introduced in the equations. Expressed in the moving system of coordinates $Ax_1x_2x_3$, the equations of motion are

$$\left[\begin{array}{c|c} \mathbf{M}_{rr} & \mathbf{M}_{re} \\ \hline \mathbf{M}_{er} & \mathbf{M}_{ee} \end{array}\right] \left\{\begin{array}{c} \ddot{\mathbf{r}} \\ \hline \ddot{\mathbf{q}} \end{array}\right\} + \left[\begin{array}{c|c} 0 & 0 \\ \hline 0 & \mathbf{C}_{ee} \end{array}\right] \left\{\begin{array}{c} \dot{\mathbf{r}} \\ \hline \dot{\mathbf{q}} \end{array}\right\} + \left[\begin{array}{c|c} 0 & 0 \\ \hline 0 & \mathbf{K}_{ee} \end{array}\right] \left\{\begin{array}{c} \mathbf{r} \\ \hline \mathbf{q} \end{array}\right\} = \left\{\begin{array}{c} \mathbf{f}_x^A + \boldsymbol{\phi}_r^T \mathscr{F} \\ \hline \boldsymbol{\phi}_e^T \mathscr{F} \end{array}\right\} \tag{3}$$

---

where

$\mathbf{M}_{rr}$ = rigid body mass matrix of appendage, including mass, static moment, and moment of inertia with respect to A (6×6)

$\mathbf{M}_{re}$ = rigid elastic coupling matrix ($6 \times n$)

$\mathbf{M}_{er}$ = transpose of $\mathbf{M}_{re}$

$$\mathbf{r} = \left\{\begin{array}{c} x_1^A \\ x_2^A \\ x_3^A \\ \alpha_1 \\ \alpha_2 \\ \alpha_3 \end{array}\right\} = \text{column of three translations of point } A \text{ and three rotations of base of appendage in } x \text{ system}$$

$$\mathbf{f}_x^A = \left\{\begin{array}{c} f_1 \\ f_2 \\ f_3 \\ t_1 \\ t_2 \\ t_3 \end{array}\right\}_x^A = \text{column of components of resultants of reaction forces and moments with respect to } A \text{ due to bus in } x \text{ system}$$

$\boldsymbol{\phi}_r = 3p \times 6$ matrix of rigid-body mode corresponding to points $P_1, P_2, \cdots, P_p$ (see Appendix C)

The variable $\mathbf{q}$ in Eq. (3) is of no direct interest, and will be eliminated; this elimination is readily made in the frequency domain. To this end, one may expand Eq. (3) and take the Fourier transform of both sides

$$\mathbf{M}_{rr} \bar{\ddot{\mathbf{r}}} + \mathbf{M}_{re} \bar{\ddot{\mathbf{q}}} = \bar{\mathbf{f}}_x^A + \boldsymbol{\phi}_r^T \bar{\mathscr{F}} \tag{4}$$

$$\mathbf{M}_{er} \bar{\ddot{\mathbf{r}}} + \mathbf{Z}^{-1} \bar{\ddot{\mathbf{q}}} = \boldsymbol{\phi}_e^T \bar{\mathscr{F}} \tag{5}$$

where the bar means Fourier transform of the time-variable functions $\ddot{\mathbf{r}}$, $\ddot{\mathbf{q}}$, $\mathbf{f}_x^A$, and $\mathscr{F}$; i.e.,

$$\{\bar{\ }\} = \int_{-\infty}^{+\infty} \{\ \} \exp(-i\omega t)\, dt \tag{6}$$

in which ω is the angular frequency, $i = (-1)^{1/2}$, and $\mathbf{Z}$ is a frequency-dependent diagonal matrix defined as follows:

$$\mathbf{Z} = \mathbf{Z}(\omega) = [\ Z_j\ ] \tag{7}$$

with

$$Z_j = \frac{\omega^2}{m_j (\omega^2 - \omega_j^2 - 2i\xi_j \omega_j \omega)} \tag{8}$$

Elimination of $\bar{\ddot{\mathbf{q}}}$ between Eqs. (4) and (5) gives

$$[\mathbf{M}_{rr} - \mathbf{M}_{re} \mathbf{Z} \mathbf{M}_{er}]\, \bar{\ddot{\mathbf{r}}} = \bar{\mathbf{f}}_x^A + [\boldsymbol{\phi}_r^T - \mathbf{M}_{re} \mathbf{Z} \boldsymbol{\phi}_e^T]\, \bar{\mathscr{F}} \tag{9}$$

B. Equations of Motion of Bus

Let $OX_1X_2X_3$ be called a system of coordinates of origin O fixed in the bus. This system will be referred to as the X system of coordinates (point O will be different from A in general). The matrix equations of motion of the bus are

$$\mathbf{M}' \bar{\ddot{\mathbf{R}}} = \bar{\mathbf{F}}_X^O - \bar{\mathbf{f}}_X^O \tag{10}$$

where

$\mathbf{M}'$ = mass matrix of bus, including mass, static moment, and moment of inertia about O

$$\mathbf{R} = \begin{Bmatrix} X_1^o \\ X_2^o \\ X_3^o \\ \theta_1 \\ \theta_2 \\ \theta_3 \end{Bmatrix} = \text{column of three translations of point } O \text{ and three rotations of bus in } X \text{ system}$$

$$\mathbf{F}_X^o = \begin{Bmatrix} F_1 \\ F_2 \\ F_3 \\ T_1 \\ T_2 \\ T_3 \end{Bmatrix} = \text{column of components of resultant of external forces and torques with respect to } O \text{ applied on bus in } OX_1X_2X_3 \text{ system}$$

$$\mathbf{f}_X^o = \begin{Bmatrix} f_1 \\ f_2 \\ f_3 \\ t_1 \\ t_2 \\ t_3 \end{Bmatrix}_X^o = \text{column of components of resultant of reaction forces and torques with respect to } O \text{ caused by appendage reactions in } OX_1X_2X_3 \text{ system}$$

C. Equations of Motion of System

To obtain the global equations of motion, one may eliminate the reaction forces between Eqs. (9) and (10). However, because different systems of coordinates are used, transformation of coordinates is necessary.

The acceleration column $\ddot{\mathbf{r}}$ of point A in the x system is related to the acceleration $\ddot{\mathbf{R}}$ of point O in the X system by

$$\ddot{\mathbf{r}} = \mathbf{B}\,\ddot{\mathbf{R}} \tag{11}$$

In Eq. (11), $\mathbf{B}$ is an orthogonal transformation matrix defined as follows:

$$\mathbf{B} = \left[\begin{array}{c|c} \mathbf{b} & \mathbf{b}\tilde{\mathbf{X}} \\ \hline 0 & \mathbf{b} \end{array}\right] \tag{12}$$

where

$$\tilde{\mathbf{X}} = \begin{bmatrix} 0 & X_3 & -X_2 \\ -X_3 & 0 & X_1 \\ X_2 & -X_1 & 0 \end{bmatrix} \tag{13}$$

is formed from the components X_1, X_2, X_3 of point A in the X system and $\mathbf{b}$ is the matrix of the direction cosines between the x and X systems.

The matrix $\mathbf{b}$ is orthogonal

$$\mathbf{b} = \begin{bmatrix} b_{11} & b_{12} & b_{13} \\ b_{21} & b_{22} & b_{23} \\ b_{31} & b_{32} & b_{33} \end{bmatrix} \tag{14}$$

for which

$$\mathbf{b}_{ij} = \cos(x_i, X_j) \tag{15}$$

where (x_i, X_j) is the angle between the x_i axis of system x with the X_j axis of system X.

Similar to those of Eq. (11), the reaction forces and moments expressed in the x and X systems are related by

$$\mathbf{f}_X^o = \mathbf{B}^T \mathbf{f}_x^A \tag{16}$$

Combining Eqs. (9), (10), (11), and (16), and eliminating the reaction forces and moments, one finally obtains

$$[\mathbf{M}' + \mathbf{B}^T[\mathbf{M}_{rr} - \mathbf{M}_{re}\mathbf{Z}\mathbf{M}_{er}]\mathbf{B}]\,\ddot{\bar{\mathbf{R}}} = \bar{\mathbf{F}}_X^o + \mathbf{B}^T[\boldsymbol{\phi}_r^T - \mathbf{M}_{re}\mathbf{Z}\,\boldsymbol{\phi}_e^T]\,\bar{\mathscr{F}} \tag{17}$$

To simplify the presentation, it is convenient to introduce two frequency-dependent matrices,

$$\mathbf{D} = \mathbf{D}(\omega) = \mathbf{M}_{rr} - \mathbf{M}_{re}\,\mathbf{Z}(\omega)\,\mathbf{M}_{er} \tag{18}$$

and

$$\mathbf{N} = \mathbf{N}(\omega) = \boldsymbol{\phi}_r^T - \mathbf{M}_{re}\mathbf{Z}(\omega)\,\boldsymbol{\phi}_e^T \tag{19}$$

Equation (17) becomes

$$[\mathbf{M}' + \mathbf{B}^T\mathbf{D}\,\mathbf{B}]\,\mathbf{R} = \mathbf{F}_x^o + \mathbf{B}^T\mathbf{N}\,\mathscr{F} \tag{20}$$

D. Equation of Motion of System With Several Appendages

If M appendages are attached to the bus, there will be a transformation matrix $\mathbf{B}_m$; matrices $\mathbf{D}_m$, $\mathbf{N}_m$, $\mathscr{F}_m$ for each appendage m; and the equation of motion for the total system will be obtained by adding each new appendage to Eq. (20); i.e., yielding

$$\left[\mathbf{M}' + \sum_{m=1}^{M} \mathbf{B}_m^T \mathbf{D}_m \mathbf{B}_m\right] \ddot{\bar{\mathbf{R}}} = \bar{\mathbf{F}}_x^o + \sum_{m=1}^{M} \mathbf{B}_m^T \mathbf{N}_m \bar{\mathscr{F}}_m \tag{21}$$

E. Structural Transfer Function for Attitude Control by Control Jets

In the case of attitude control by cold gas jets, the jets (or thrusters) occur in pairs to apply forces on the bus or the appendages that are equal and opposite so that pure torques will be produced. It will be assumed that the control is made about the three axes OX_1,OX_2,OX_3 (i.e., the thrusters apply control forces F_1, $-F_1$, F_2, $-F_2$, F_3, $-F_3$, which one may express in vehicle coordinates $OX_1X_2X_3$). Therefore, the right side of Eq. (21) can be expressed in terms of only three parameters F_1,F_2,F_3:

$$\bar{\mathbf{F}}_x^o + \sum_{m=1}^{M} \mathbf{B}_m^T \mathbf{N}_m \bar{\mathscr{F}}_m = \mathbf{Q}(\omega)\, \bar{\mathbf{F}} \tag{22}$$

where

$$\bar{\mathbf{F}} = \begin{Bmatrix} \bar{F}_1 \\ \bar{F}_2 \\ \bar{F}_3 \end{Bmatrix}$$

and $\mathbf{Q}(\omega)$ is a 6×3 frequency-dependent matrix that is dependent upon the location of the control forces. An expression of $\mathbf{Q}(\omega)$ is given in Appendix A, Eqs. (A-7)–(A-10).

If the matrix premultiplying R is called $\mathbf{H}$,

$$\mathbf{H} = \mathbf{H}(\omega) = \mathbf{M}' + \sum_{m=1}^{M} \mathbf{B}_m^T \mathbf{D}_m \mathbf{B}_m \tag{23}$$

then Eq. (21) becomes

$$\mathbf{H}\, \ddot{\bar{\mathbf{R}}} = \mathbf{Q}\, \bar{\mathbf{F}} \tag{24}$$

The translations X_1^o,X_2^o,X_3^o are now eliminated from Eq. (24). To this end, the following partitioning is done:

$$\ddot{\mathbf{R}} = \begin{Bmatrix} \ddot{\mathbf{X}} \\ \ddot{\bar{\theta}} \end{Bmatrix}, \qquad \ddot{\mathbf{X}} = \begin{Bmatrix} \ddot{X}_1^o \\ \ddot{X}_2^o \\ \ddot{X}_3^o \end{Bmatrix}, \qquad \ddot{\bar{\theta}} = \begin{Bmatrix} \ddot{\theta}_1 \\ \ddot{\theta}_2 \\ \ddot{\theta}_3 \end{Bmatrix} \tag{25}$$

$$\mathbf{H} = \left[\begin{array}{c|c} \mathbf{H}_{XX} & \mathbf{H}_{X\theta} \\ \hline \mathbf{H}_{\theta X} & \mathbf{H}_{\theta\theta} \end{array}\right], \qquad \mathbf{Q} = \left[\begin{array}{c} \mathbf{Q}_X \\ \hline \mathbf{Q}_\theta \end{array}\right] \tag{26}$$

Finally, the attitude-angle accelerations $\ddot{\theta}_1$,$\ddot{\theta}_2$,$\ddot{\theta}_3$ are related to the forces F_1,F_2,F_3 by

$$[\mathbf{H}_{\theta\theta} - \mathbf{H}_{\theta X} \mathbf{H}_{XX}^{-1} \mathbf{H}_{X\theta}]\, \ddot{\bar{\theta}} = [\mathbf{Q}_\theta - \mathbf{H}_{\theta X} \mathbf{H}_{XX}^{-1} \mathbf{Q}_X]\, \bar{\mathbf{F}} \tag{27}$$

The right side of Eq. (27) is equivalent to a torque $\bar{\mathbf{T}}$ applied to the structure; i.e.,

$$[\mathbf{Q}_\theta - \mathbf{H}_{\theta X} \mathbf{H}_{XX}^{-1} \mathbf{Q}_X]\, \bar{\mathbf{F}} = \bar{\mathbf{T}} \tag{28}$$

or

$$\mathbf{P}\, \bar{\mathbf{F}} = \bar{\mathbf{T}} \tag{29}$$

where

$$\mathbf{P}(\omega) = \mathbf{P} = [\mathbf{Q}_\theta - \mathbf{H}_{\theta X} \mathbf{H}_{XX}^{-1} \mathbf{Q}_X] \tag{30}$$

In addition, the angular accelerations $\ddot{\bar{\theta}}$ are related to the angles $\bar{\theta}$ by

$$\ddot{\bar{\theta}} = -\omega^2\, \bar{\theta} \tag{31}$$

Therefore,

$$\bar{\theta} = \mathbf{Y}\, \bar{\mathbf{T}} \tag{32}$$

where

$$\mathbf{Y} = [\omega^2 \mathbf{H}_{\theta\theta} - \omega^2 \mathbf{H}_{\theta X} \mathbf{H}_{XX}^{-1} \mathbf{H}_{X\theta}]^{-1} \tag{33}$$

F. Equations of Motion of Controlled Spacecraft

The control loop on the structure (Fig. 3) may now be introduced, with the assumption that the attitude sensors are actuated by the angles $\bar{\theta}$. The angles $\bar{\theta}$ are then fed into a control system, which has a transfer-function matrix $\mathbf{S}(\omega)$, to produce the three thruster parameters $\bar{\mathbf{F}}$ applied at given locations of the structure:

$$\bar{\mathbf{F}} = -\mathbf{S}(\omega)\, \bar{\theta} \tag{34}$$

Then the thruster parameters $\bar{\mathbf{F}}$ are transformed into a control torque $\bar{\mathbf{T}}_c$ by the thruster location matrix $\mathbf{P}(\omega)$:

$$\bar{\mathbf{T}}_c = \mathbf{P}(\omega)\, \bar{\mathbf{F}} \tag{35}$$

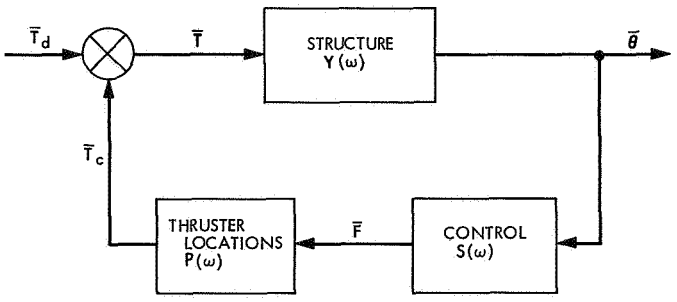

Fig. 3. Attitude control loop

If it is now assumed that there exists an external disturbance-torque column $\bar{\mathbf{T}}_d$, that acts on the whole system, the torque $\bar{\mathbf{T}}$ is the sum of $\bar{\mathbf{T}}_c$ and $\bar{\mathbf{T}}_d$, and Eq. (28) may be rewritten as

$$\bar{\boldsymbol{\theta}} = \mathbf{Y}\{\bar{\mathbf{T}}_c + \bar{\mathbf{T}}_d\} \tag{36}$$

Using Eqs. (34) and (35), one finally obtains

$$\bar{\boldsymbol{\theta}} = [\mathbf{1} + \mathbf{YPS}]^{-1}\mathbf{Y}\bar{\mathbf{T}}_d \tag{37}$$

where $\mathbf{1}$ is the unit matrix. Equation (36) is a generalization of the classical one-dimensional control equation for a tridimensional elastic spacecraft. Because $\mathbf{Y}$ is not obtained directly, but through an inversion, it is more practical to rewrite Eq. (37) for numerical computation as follows:

$$\bar{\boldsymbol{\theta}} = \mathscr{H}\bar{\mathbf{T}}_d \tag{38}$$

where

$$\mathscr{H} = [\omega^2\mathbf{H}_{\theta X}\mathbf{H}_{XX}^{-1}\mathbf{H}_{X\theta} - \omega^2\mathbf{H}_{\theta\theta} + \mathbf{PS}]^{-1} \tag{39}$$

G. Computation of Control Matrix S(ω)

Each term of the control matrix $\mathbf{S}(\omega)$ is expressed as a ratio of products of second-order polynomials in ω; i.e.,

$$S_{jk} = K_{jk}\frac{\prod_{l=1}^{L}(\gamma_l^{jk} - \alpha_l^{jk}\omega^2 + i\beta_l^{jk}\omega)}{\prod_{m=1}^{M}(\eta_m^{jk} - \delta_m^{jk}\omega^2 + i\epsilon_m^{jk}\omega)}$$

$$j,k = 1,2,3 \tag{40}$$

where α_l^{jk}, β_l^{jk}, γ_l^{jk}, δ_m^{jk}, ϵ_m^{jk}, and η_m^{jk} are coefficients obtained from the control circuits and K_{jk} is the gain of each loop or coupling loop of the control circuits. This expression requires that the transfer function of the control loop be computed in terms of second-order polynomials. If one term is of the first order, then the coefficient of the term in ω^2 is set equal to zero.

H. Response to a Disturbance Torque

Equation (38) can be used to study the response to any disturbance-torque time history $\mathbf{T}_d(t)$. The procedure is to compute numerically the Fourier transform $\bar{\mathbf{T}}_d(\omega)$ of the time history.

$$\bar{\mathbf{T}}_d(\omega) = \int_{-\infty}^{+\infty}\mathbf{T}_d(t)\exp(-i\omega t)\,dt \tag{41}$$

for a range of frequencies $\omega = 2\pi f$, where f is the frequency in Hz. The Fourier transform column $\bar{\mathbf{T}}_d(\omega)$ is then premultiplied by the transfer-function matrix $\mathscr{H}(\omega)$ computed for the same range of frequencies, according to Eq. (38), to obtain the Fourier transform of the response; i.e., the orientation of the bus $\bar{\boldsymbol{\theta}}(\omega)$. Finally, the time history of the response is obtained by inverse transformation:

$$\boldsymbol{\theta}(t) = \frac{1}{2\pi}\int_{-\infty}^{+\infty}\bar{\boldsymbol{\theta}}(\omega)\exp(i\omega t)\,d\omega \tag{42}$$

I. Stability Study by Unit-Impulse Response

The instability (if any) will be evidenced by the computation of the response, as shown in Eq. (42). However, a special type of excitation can be chosen; namely, the unit impulse. To this end, a delta function $\delta(t)$, which is infinite for $t = 0$ and zero for $t \neq 0$, is used as a disturbance torque on each direction in turn. For example:

$$\mathbf{T}_d(t) = \begin{Bmatrix}\delta(t)\\0\\0\end{Bmatrix} \tag{43}$$

The Fourier transform of these torques is then

$$\bar{\mathbf{T}}_d(\omega) = \begin{Bmatrix}1\\0\\0\end{Bmatrix} \tag{44}$$

and the Fourier transform of the control angles is

$$\bar{\boldsymbol{\theta}}(\omega) = \begin{Bmatrix}\mathscr{H}_{11}\\\mathscr{H}_{21}\\\mathscr{H}_{31}\end{Bmatrix} = \mathscr{H}_1 \tag{45}$$

where $\mathscr{H}_1$ is the first column of transfer-function matrix $\mathscr{H}(\omega)$. The corresponding time histories of the responses are

$$\begin{Bmatrix} \theta_1(t) \\ \theta_2(t) \\ \theta_3(t) \end{Bmatrix} = \mathbf{h}_1(t) = \frac{1}{2\pi}\int_{-\infty}^{+\infty} \mathscr{H}_1(\omega) \exp(i\omega t)\, d\omega \tag{46}$$

Responses corresponding to unit-impulse torques $T_{d_2} = \delta(t)$ and $T_{d_3} = \delta(t)$ are obtained in the same manner. The result is that a response to the unit-impulse matrix $\mathbf{h}(t)$ corresponds to the transfer-function matrix $\mathscr{H}$:

$$\mathbf{h}(t) = \begin{bmatrix} h_{11}(t) & h_{12}(t) & h_{13}(t) \\ h_{21}(t) & h_{22}(t) & h_{23}(t) \\ h_{31}(t) & h_{32}(t) & h_{33}(t) \end{bmatrix} \tag{47}$$

with

$$h_{\alpha\beta}(t) = \frac{1}{2\pi}\int_{-\infty}^{+\infty} \mathscr{H}_{\alpha\beta} \exp(i\omega t)\, d\omega \qquad \alpha, \beta = 1,2,3 \tag{48}$$

The matrix $\mathbf{h}(t)$ is a symmetric matrix

$$h_{\alpha\beta}(t) = h_{\beta\alpha}(t) \tag{49}$$

The display of the time history of the terms $h_{\alpha\beta}(t)$ of the matrix $\mathbf{h}(t)$ provides a criterion for the stability of the system by direct inspection (Fig. 4). The system is:

(1) Stable if all $h_{\alpha\beta}(t) \to 0$ for $t \to \infty$.

(2) Unstable if any $h_{\alpha\beta}(t) \to \infty$ for $t \to \infty$.

J. Programming

The method outlined herein has been programmed on a timeshare digital computer terminal. The FORTRAN II language was used, and the plotting was done directly at the terminal site.

The main functions of the program are to:

(1) Compute the transfer-function matrix $\mathscr{H}(\omega)$ for a range of frequencies ω and a range of gains K_{jk} in accordance with Eq. (39).

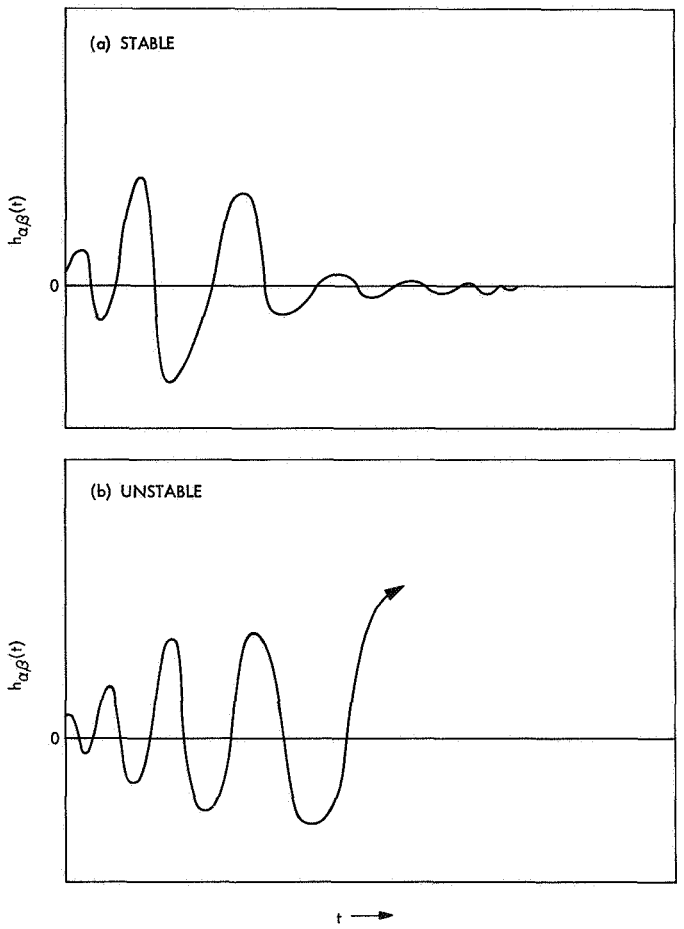

Fig. 4. Graphs of system stability in terms of unit-impulse response: (a) stable; (b) unstable

(2) Plot the modulus and phase angle of each term $\mathscr{H}_{\alpha\beta}(\omega)$ of the matrix $\mathscr{H}(\omega)$:

$$\mathscr{M}_{\alpha\beta} = (A_{\alpha\beta}^2 + B_{\alpha\beta}^2)^{1/2} \tag{50a}$$

$$\psi_{\alpha\beta} = \tan^{-1}\frac{B_{\alpha\beta}}{A_{\alpha\beta}} \tag{50b}$$

$$\mathscr{H}_{\alpha\beta}(\omega) = A_{\alpha\beta} + iB_{\alpha\beta} \tag{50c}$$

(3) Compute the inverse transfer function of each term of the matrix $\mathscr{H}(\omega)$ to give the impulse-response matrix $\mathbf{h}(t)$ in accordance with Eq. (48).

(4) Plot each term of $\mathbf{h}(t)$ as a function of time.

The program can handle a maximum of 10 appendages, each having a maximum of 20 normal modes. The maximum number of terms in the numerator and the denominator of the control loops is 10.

The inverse Fourier transforms are computed using the fast Fourier transform algorithm of Cooley and Tukey (Ref. 4), as is shown in Appendix B.

1. Computation of determinant. In addition, the program can compute the determinant of the inverse of $\mathcal{H}(\omega)$:

$$\Delta(\omega) = \left| \omega^2 \mathbf{H}_{\theta X} \mathbf{H}_{XX}^{-1} \mathbf{H}_{X\theta} - \omega^2 \mathbf{H}_{\theta\theta} + \mathbf{PS} \right| \qquad (51)$$

This determinant is zero for a certain value of frequency ω when the system is at the limit between stability and instability because the damping is zero for this frequency. For display purposes, it is more significant to plot the inverse of the determinant $\Delta(\omega)$ and also to normalize this inverse. To this end, a new function $R(\omega)$ is defined as follows:

$$R(\omega) = \frac{\overset{*}{K}_{11}\overset{*}{K}_{22}\overset{*}{K}_{33}}{\Delta(\omega)} \qquad (52)$$

where $\overset{*}{K}_{11}$, $\overset{*}{K}_{22}$, $\overset{*}{K}_{33}$ are the product of the diagonal gains K_{11}, K_{22}, K_{33} by the moment arms d_{11}, d_{22}, d_{33} of the three thrusters with respect to O. That is,

$$\overset{*}{K}_{ii} = K_{ii}\, d_{ii}, \qquad i = 1,2,3 \qquad (53)$$

An infinite peak of the modulus of $R(\omega)$ indicates instability at the frequency of that peak. The corresponding time history $r(t)$ is also computed by inverse Fourier transform. The display of $r(t)$ will indicate instability if $r(t)$ is infinitely increasing with time. This latter method saves the computation of unit responses $h_{\alpha\beta}(t)$ if only stability is of interest.

2. Example of application of method. The method has been applied to an idealized spacecraft consisting of a 400-lb bus with two appendages having arbitrary orientation (Figs. 5 and 6). Appendage 1 weighs 200 lb; appendage 2 weighs 300 lb. Each appendage has 8 degrees of freedom, and the cantilevered normal modes have been calculated. The natural frequencies are listed in Table 1. These frequencies are in the range of the frequencies of the control loops. A modal damping of 1.5% was chosen for all modes.

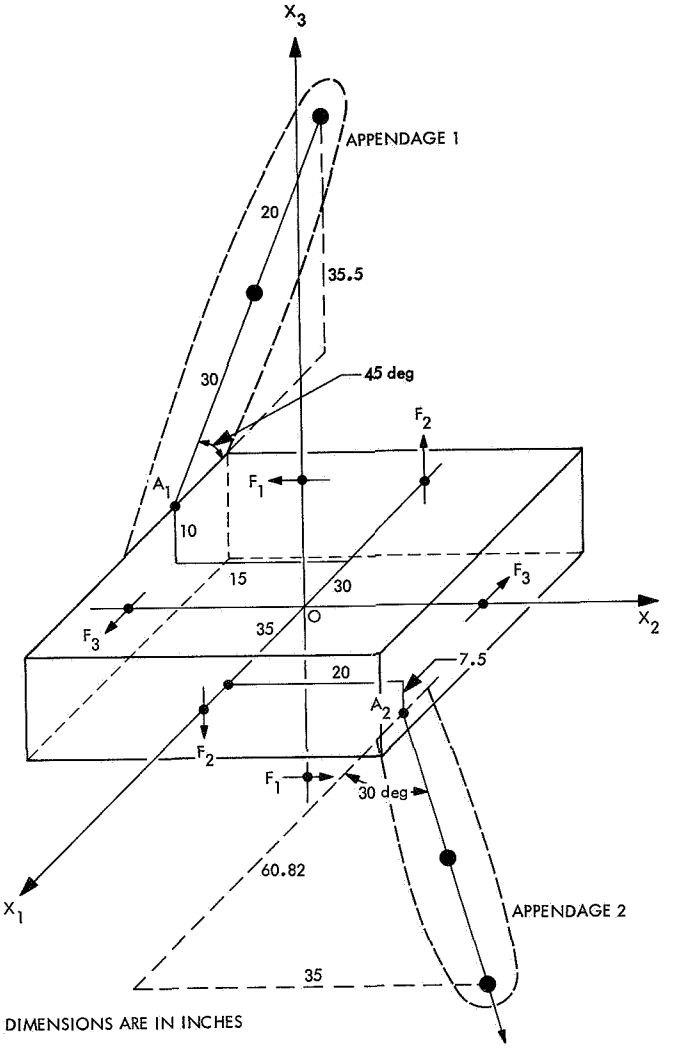

Fig. 5. Idealized spacecraft with control jets on bus only

The control circuit was assumed to be the same for the three axes of control. No control-loop cross coupling was considered. The following law was chosen

$$S_{jk} = \frac{K_{jk}(1 + 1.77\, i\omega)}{(1 + 0.111\, i\omega)(1 - 0.00013\, \omega^2 + 0.008\, i\omega)(1 - 0.0036\, \omega^2 + 0.63\, i\omega)}$$

$$j = k = 1,2,3 \qquad (54)$$

for each control loop in the three directions.

Table 1. Natural frequencies of appendages

Appendage	Natural frequency, Hz			
1	0.0526	0.06965	0.4573	0.5015
2	0.0489	0.0649	0.4100	0.4471

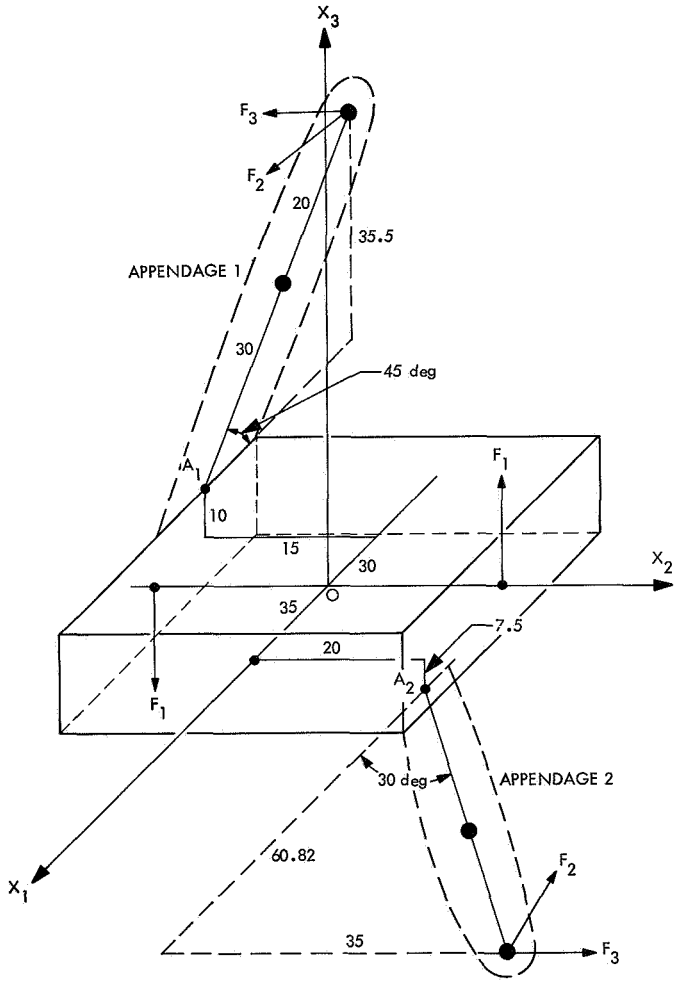

DIMENSIONS ARE IN INCHES

Fig. 6. Idealized spacecraft with control jets on bus and appendages

Two cases were investigated for stability and response.

In the first case, the control thrusters were placed on the rigid bus, as shown in Fig. 5. The same gain,

$$K = K_{11} = K_{22} = K_{33} \tag{55}$$

was taken for the three directions of control. The response $\mathbf{h}(t)$ to unit-impulse torques in the three directions was computed for different gains K. No instability was found. The time histories of the response are indicated in Figs. 7–12 for $K = 60$, and clearly show that the system is stable for this gain.

In the second case, two pairs of thrusters were placed on the tip of the appendages, as shown in Fig. 6, and the response to unit-impulse torques was studied for a range of $\overset{*}{K}_{jk}$ rather than the gain K_{jk} as defined in Eq. (53). An instability was found for $\overset{*}{K}_{11} = \overset{*}{K}_{22} = \overset{*}{K}_{33} = 1400$, which corresponds to $K_{11} = 40$, $K_{22} = 20$, $K_{33} = 8.65$, respectively. The time histories of the response are indicated in Figs. 13–18, and clearly show the instability.

In addition, plots of the modulus and phase angle of $R(\omega)$, the normalized inverse of the determinant $\Delta(\omega)$, are shown in Figs. 19 and 20, respectively. The corresponding inverse Fourier transform is shown in Fig. 21. The plot of Fig. 19 shows a very large peak, which indicates the instability occurring at the frequency of the peak; i.e., 0.08 Hz. The corresponding time history (see Fig. 16) also indicates instability.

III. Conclusions

The two examples mentioned earlier show that the frequency-domain approach is a valid method for determining the stability of the attitude control of spacecraft with large, flexible appendages. The two advantages of the method are: (1) a large number of modes of vibration can be taken for the appendages and (2) the time history of the response can be easily calculated. This response is of particular interest in the determination of the pointing accuracy.

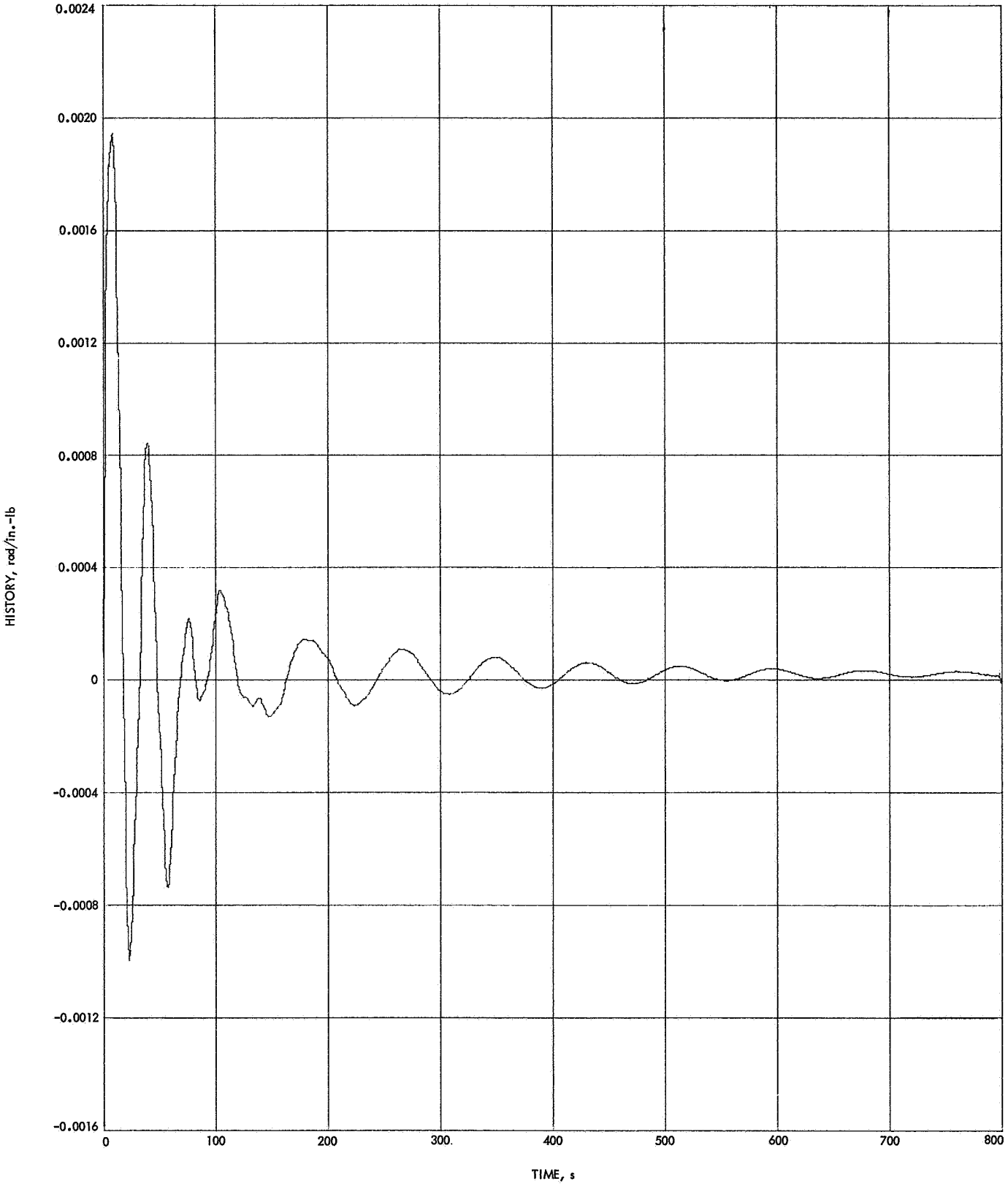

Fig. 7. Time history of $h_{11}(t)$, case 1

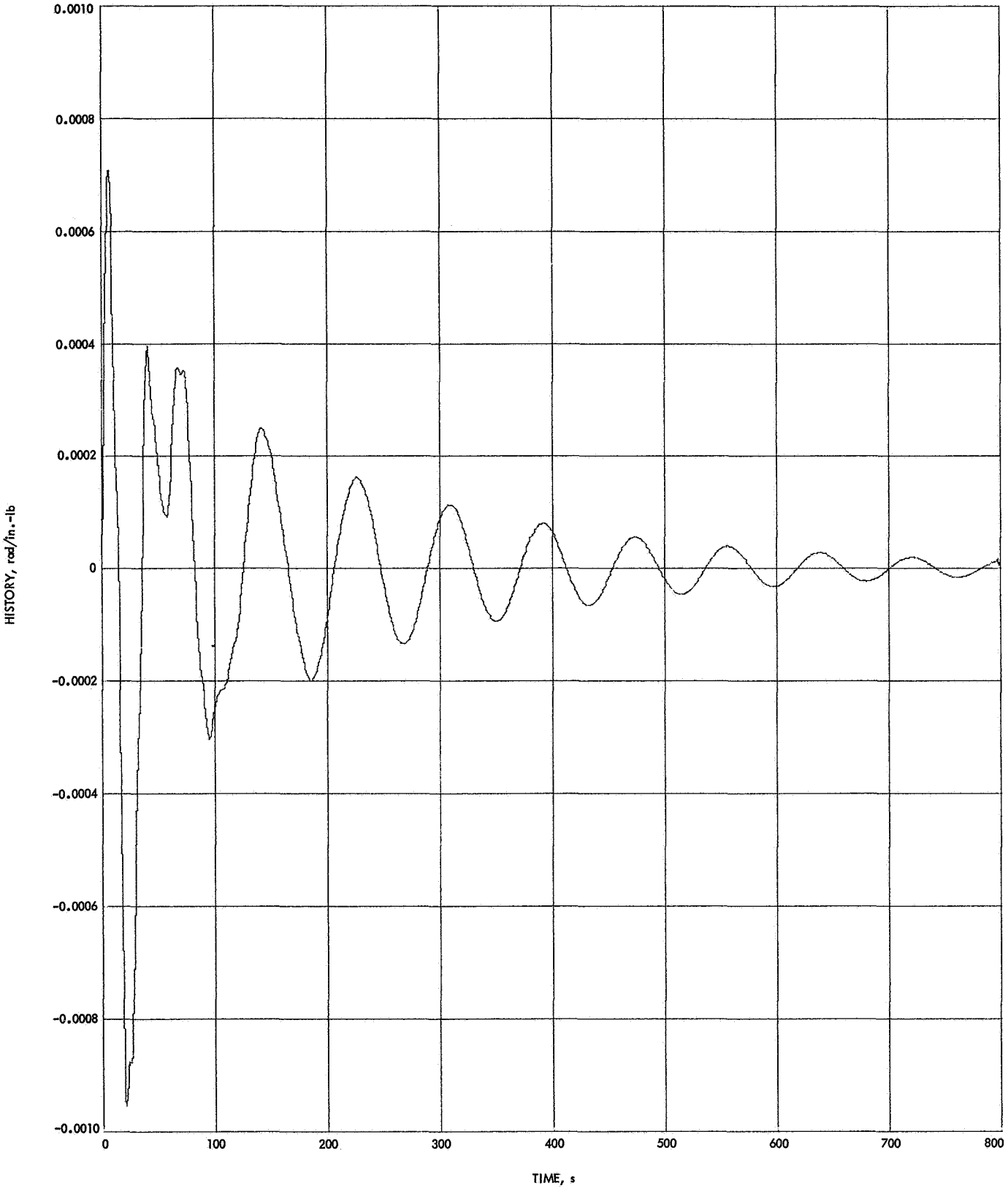

Fig. 8. Time history of $h_{12}(t)$, case 1

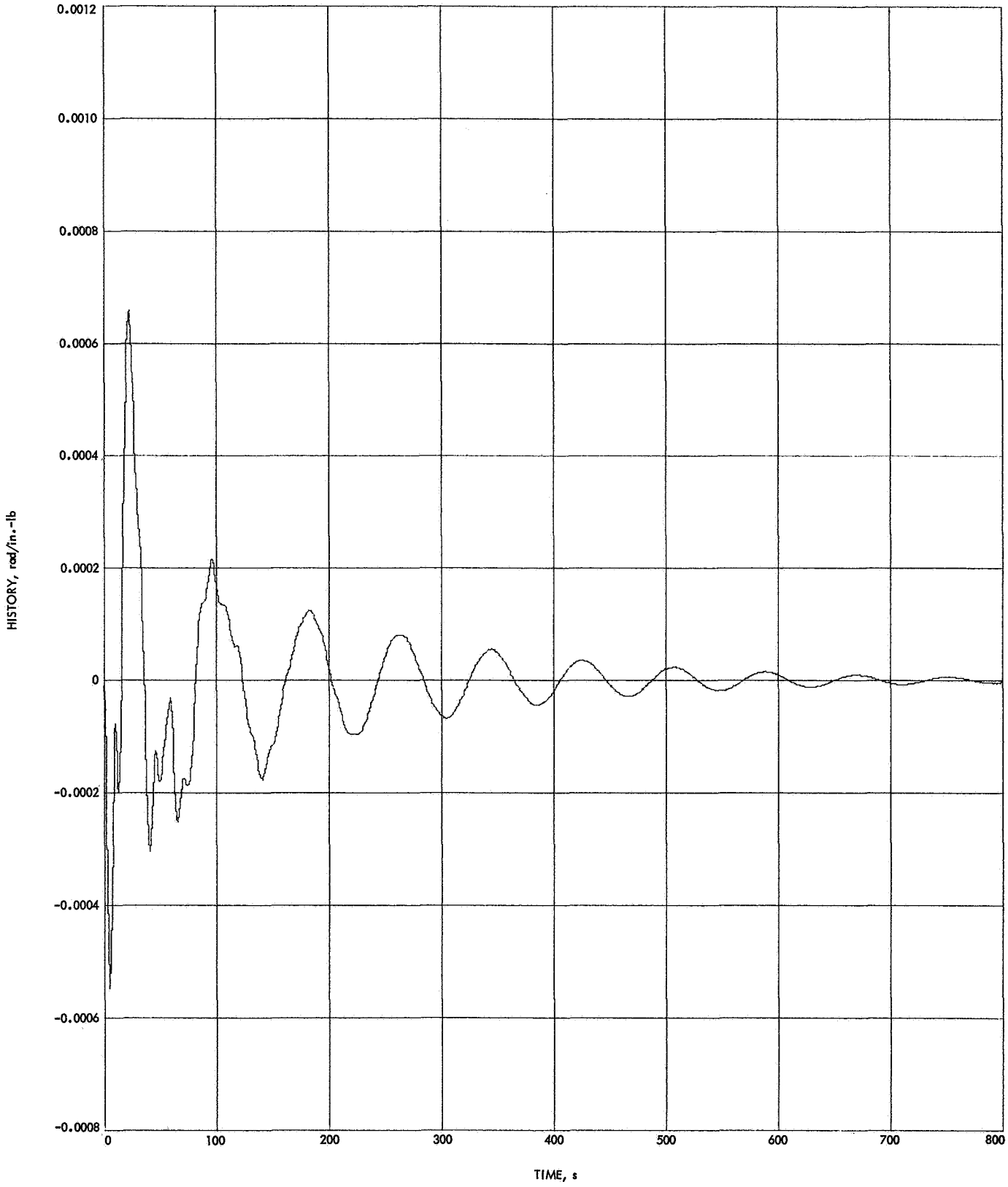

Fig. 9. Time history of $h_{13}(t)$, case 1

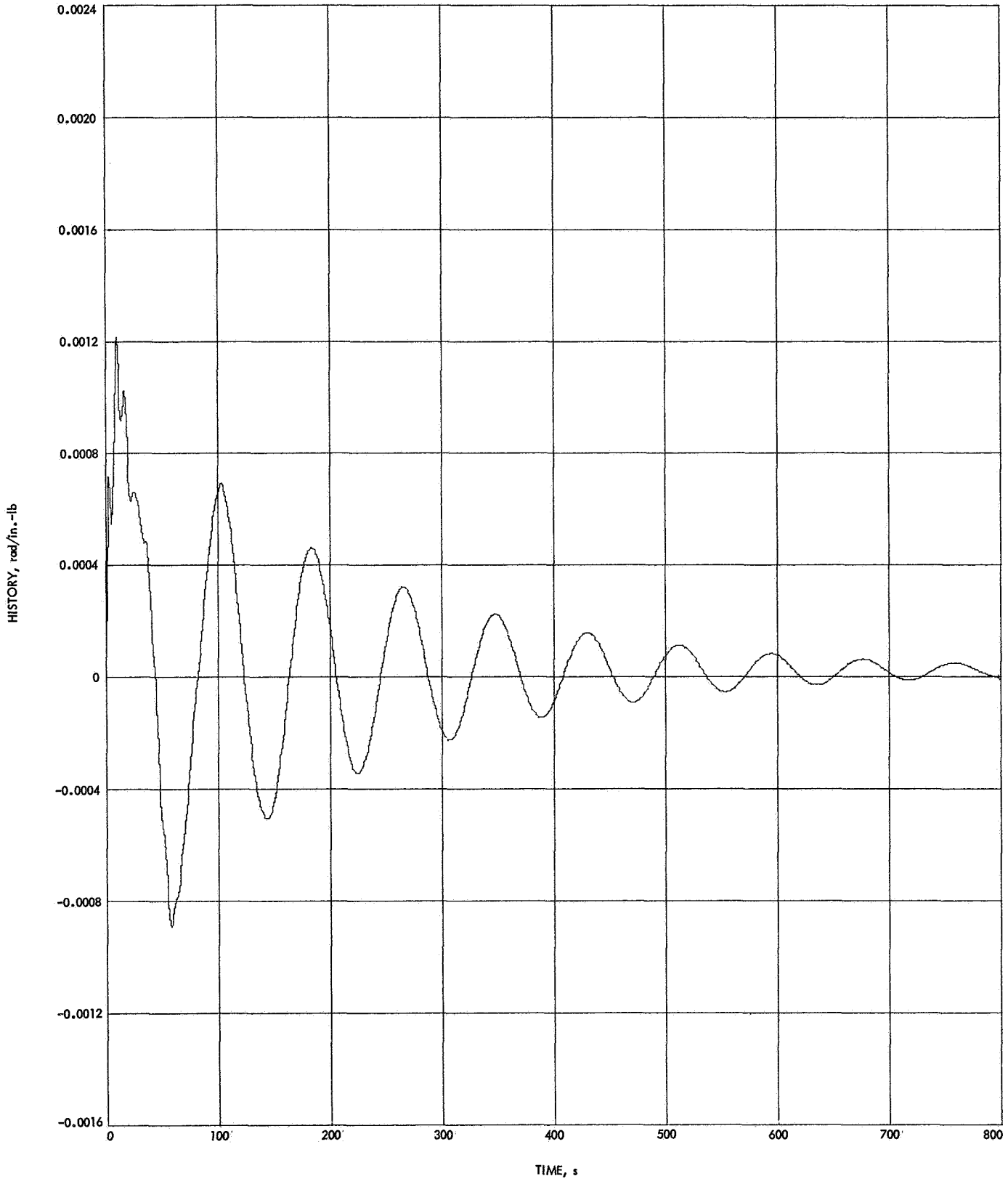

Fig. 10. Time history of $h_{22}(t)$, case 1

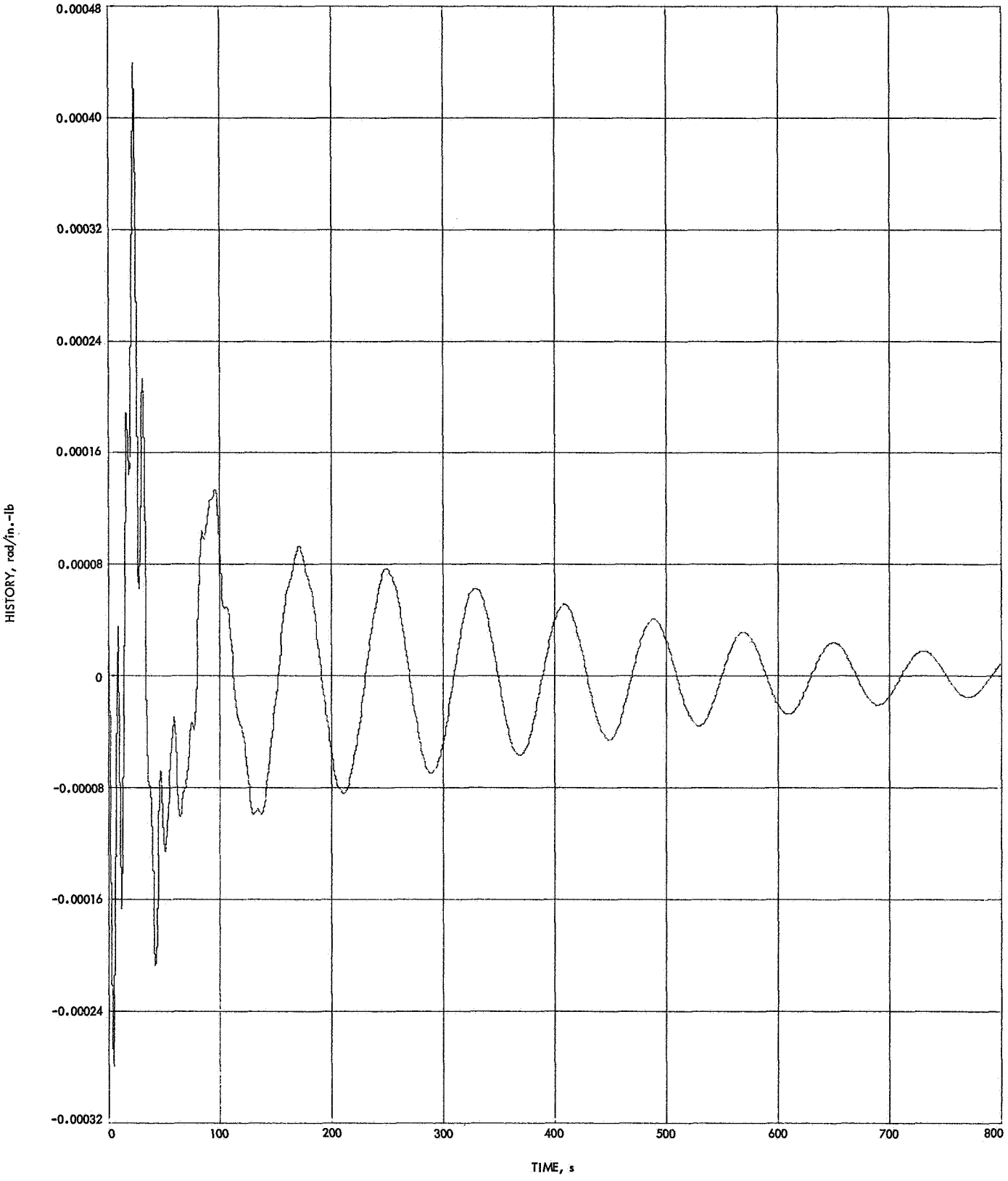

Fig. 11. Time history of $h_{23}(t)$, case 1

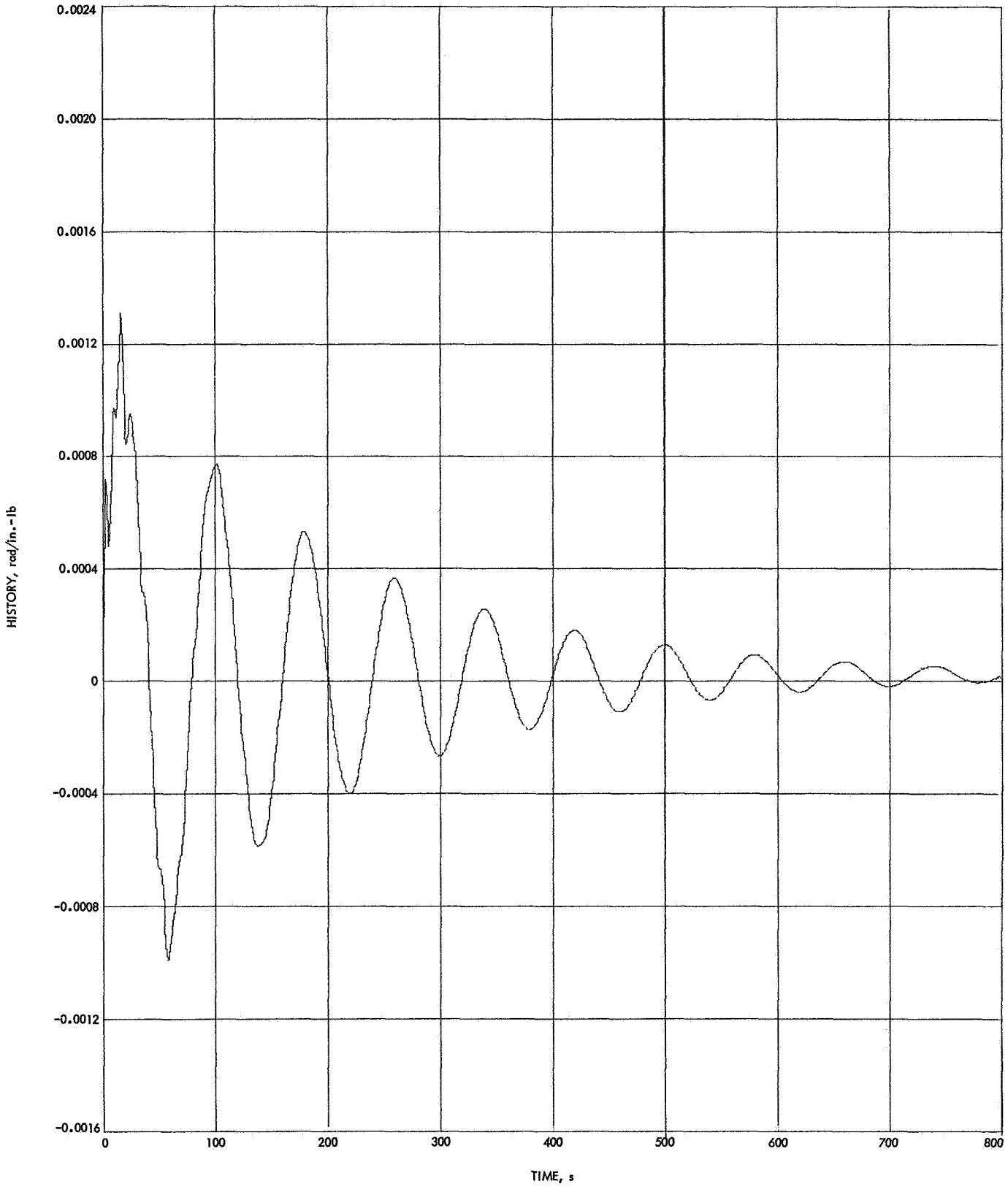

Fig. 12. Time history of $h_{33}(t)$, case 1

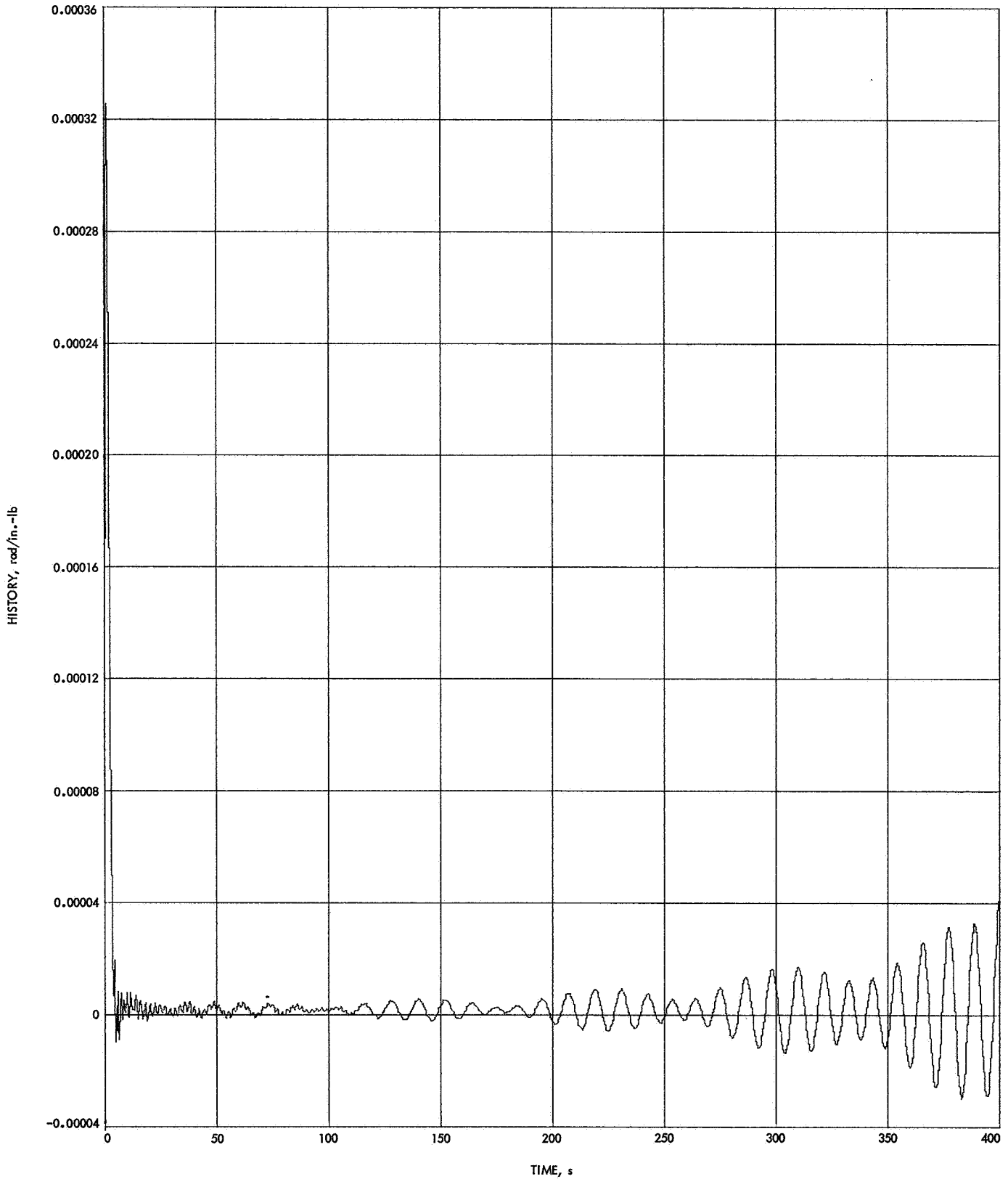

Fig. 13. Time history of $h_{11}(t)$, case 2

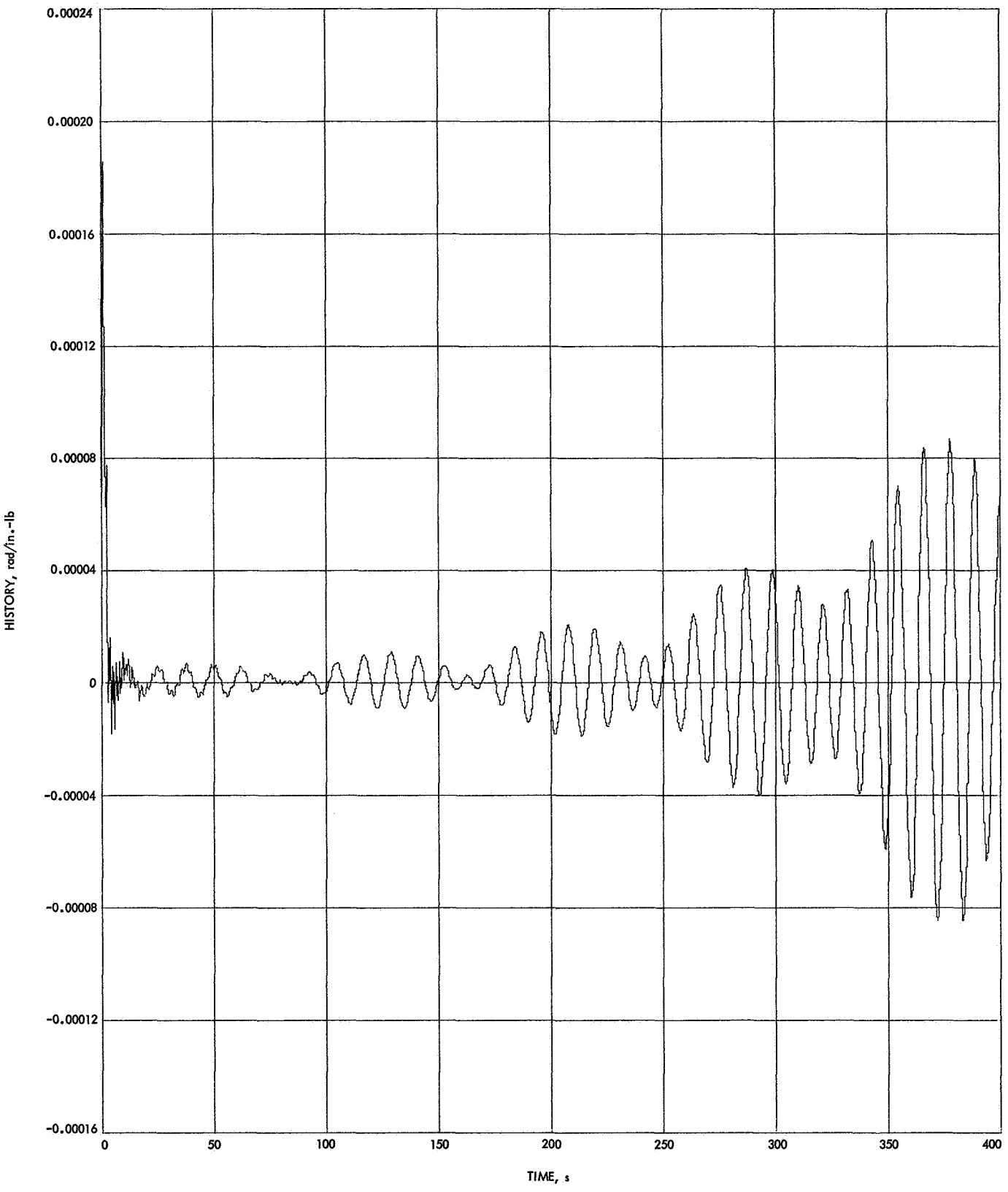

Fig. 14. Time history of $h_{12}(t)$, case 2

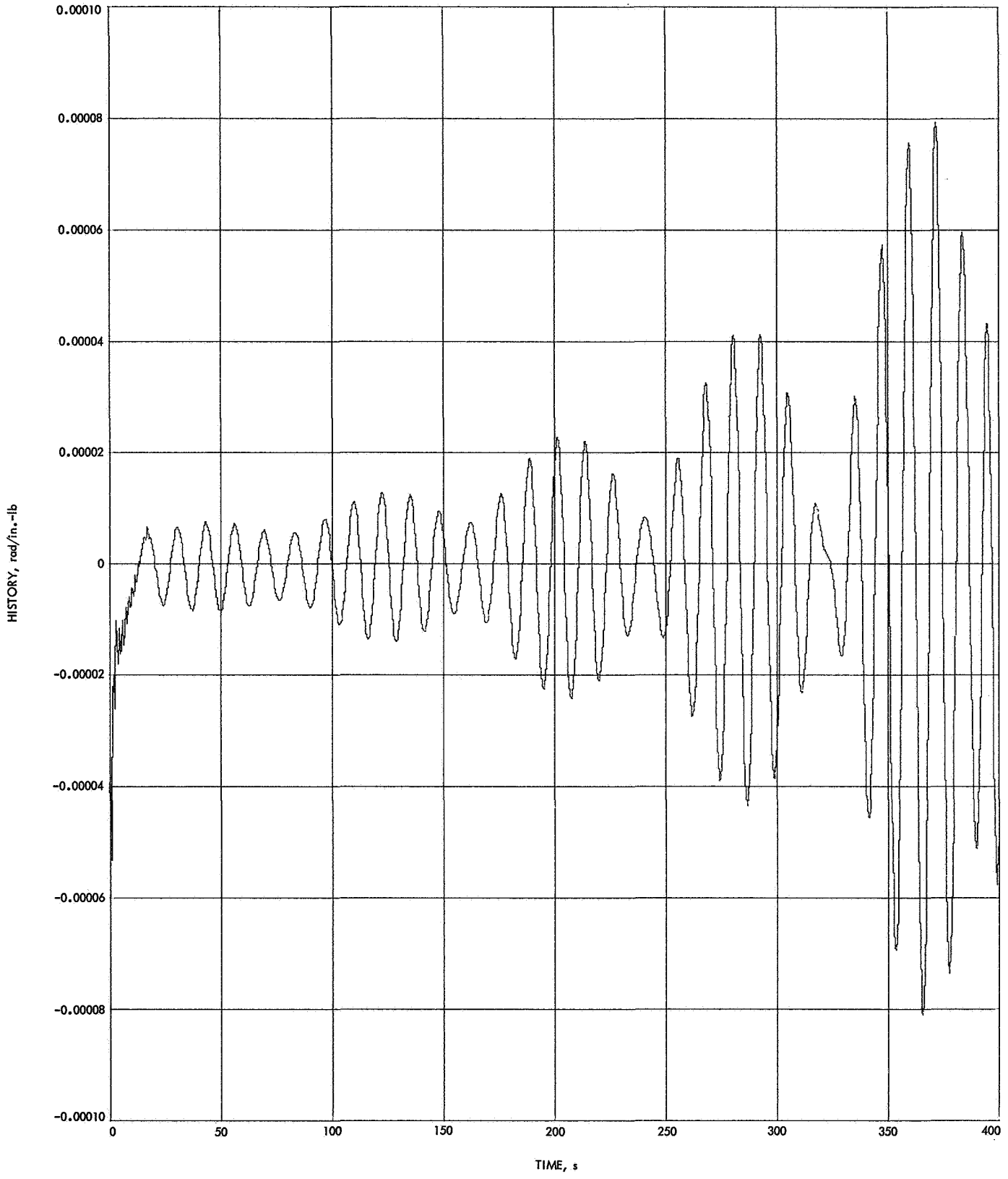

Fig. 15. Time history of $h_{13}(t)$, case 2

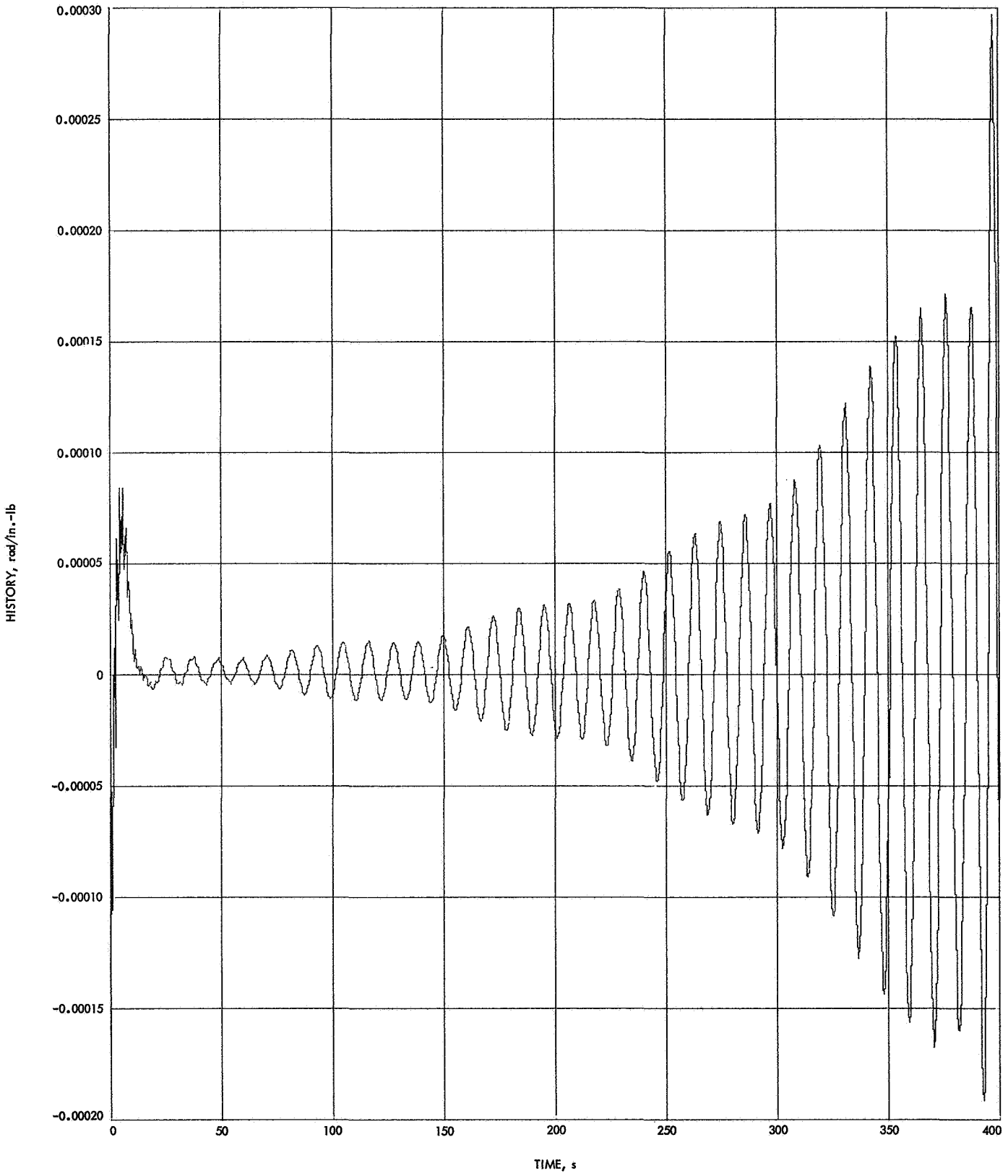

Fig. 16. Time history of $h_{22}(t)$, case 2

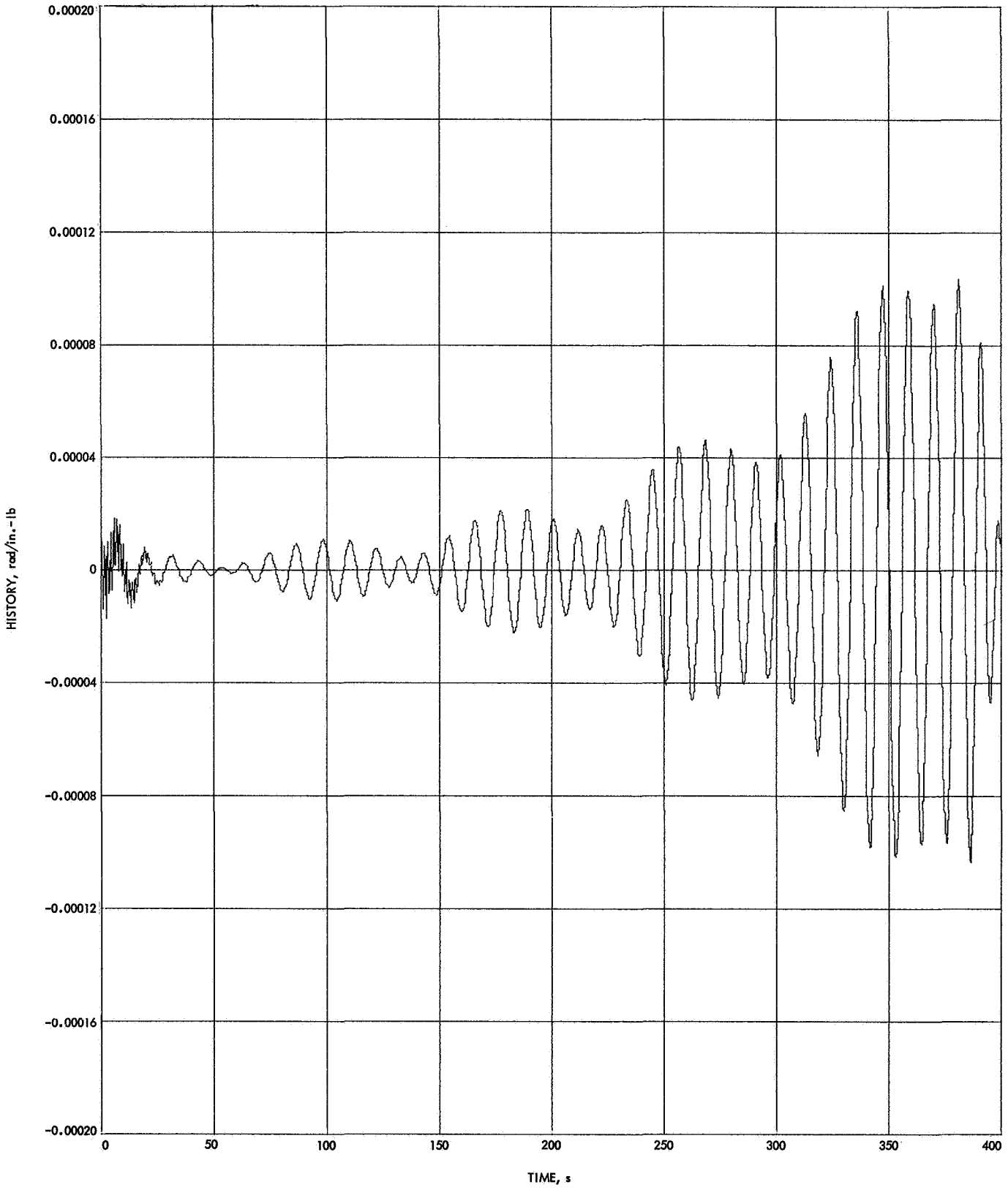

Fig. 17. Time history of $h_{23}(t)$, case 2

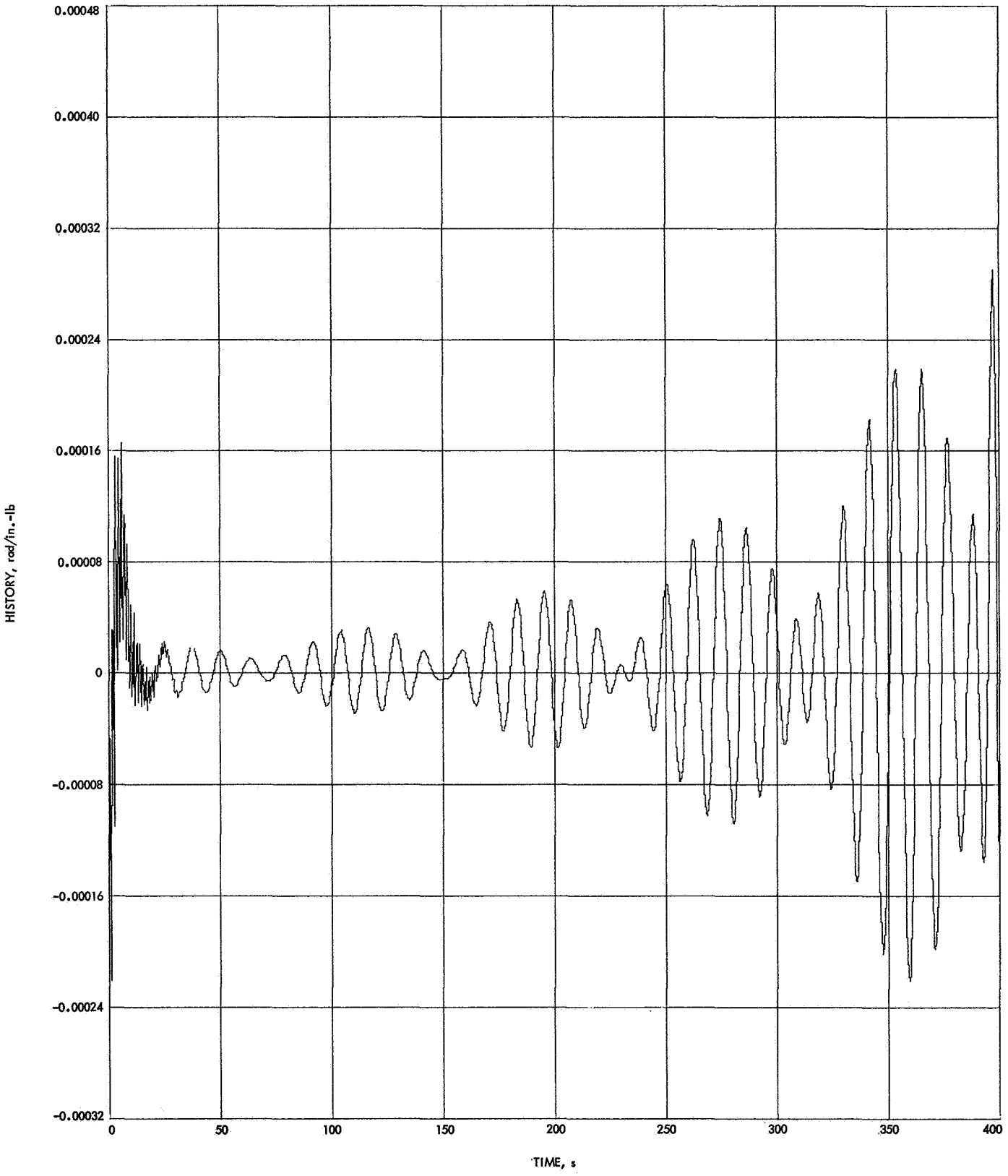

Fig. 18. Time history of $h_{33}(t)$, case 2

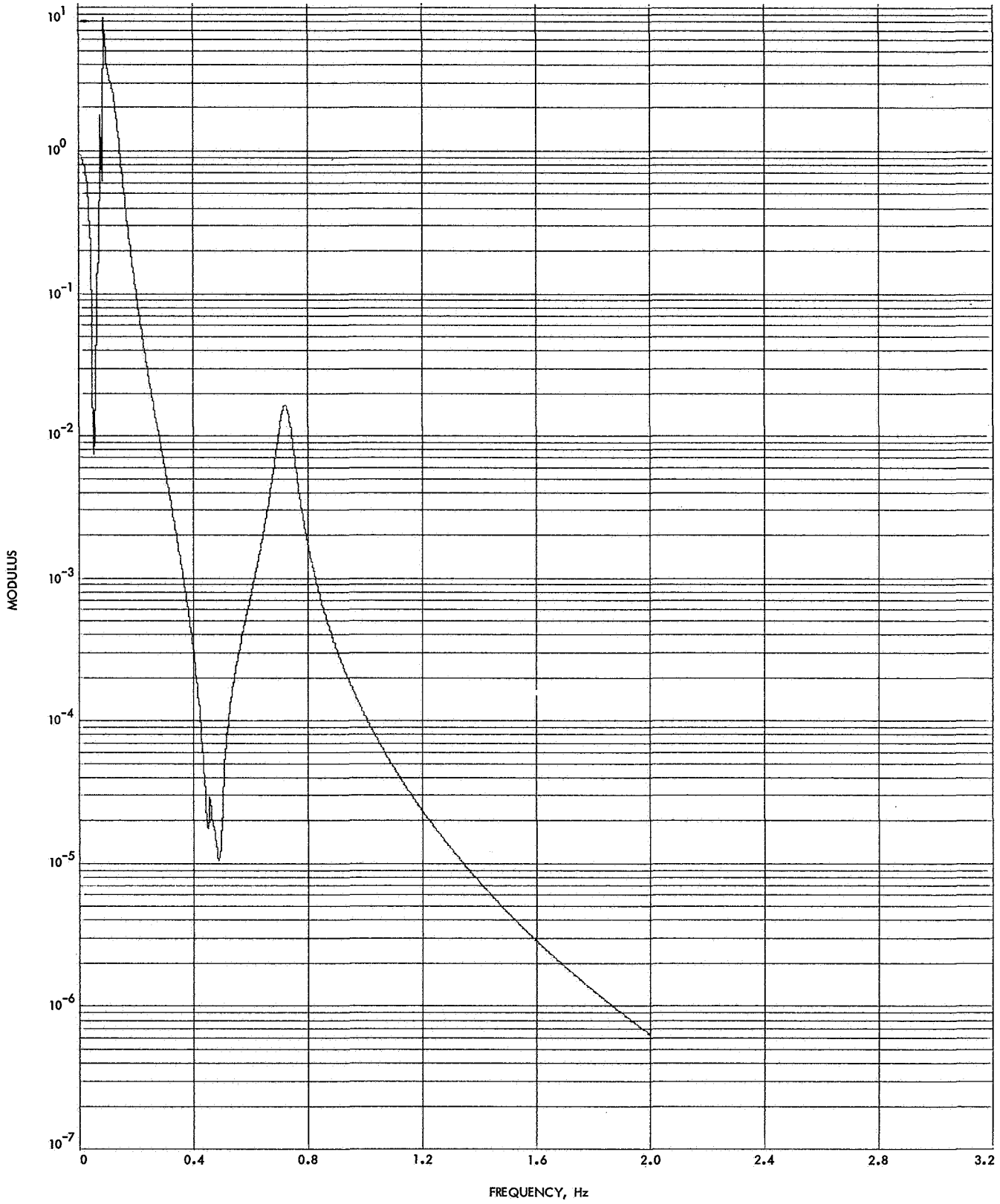

Fig. 19. Modulus of inverse of determinant, case 2

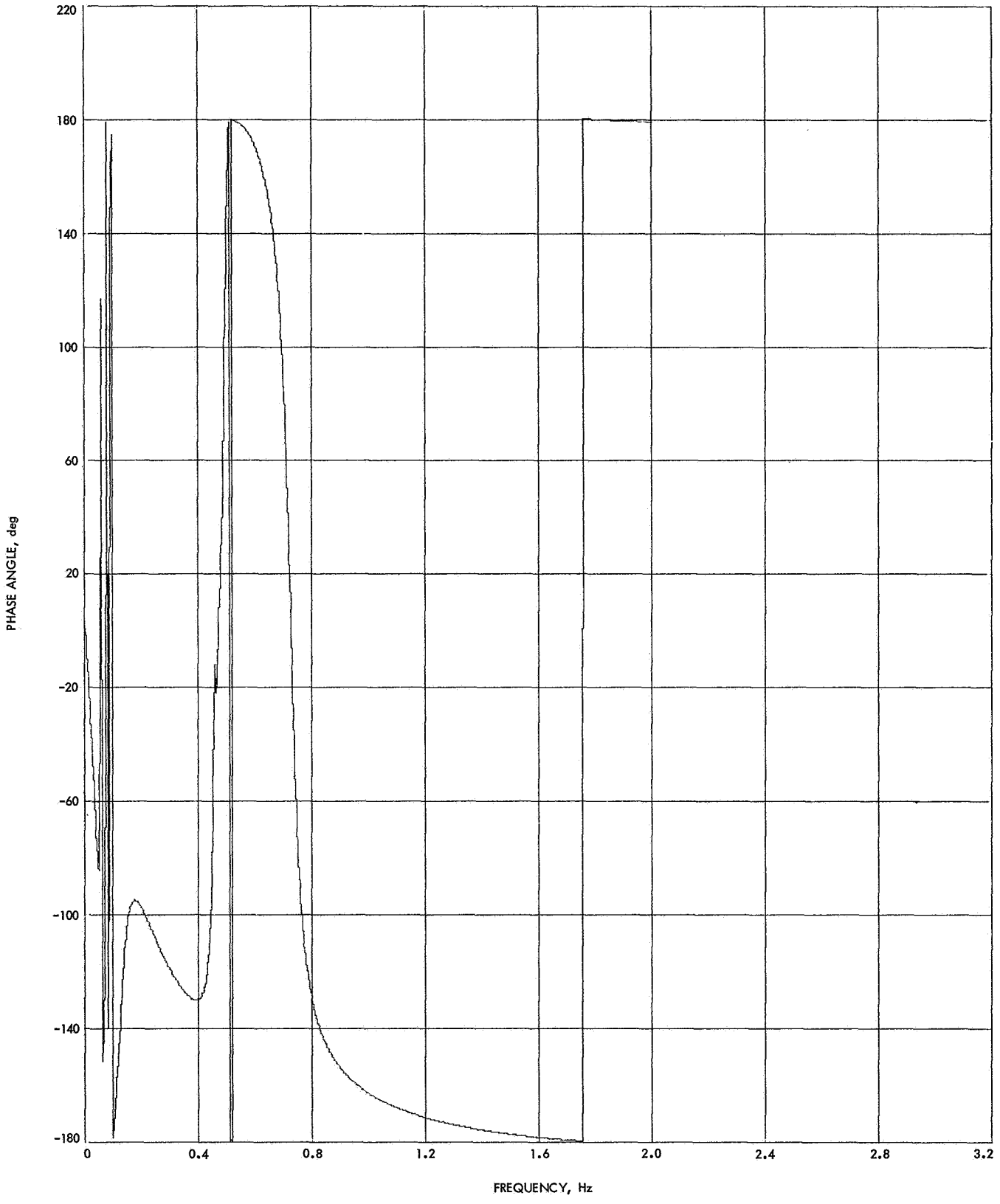

Fig. 20. Phase angle of inverse of determinant, case 2

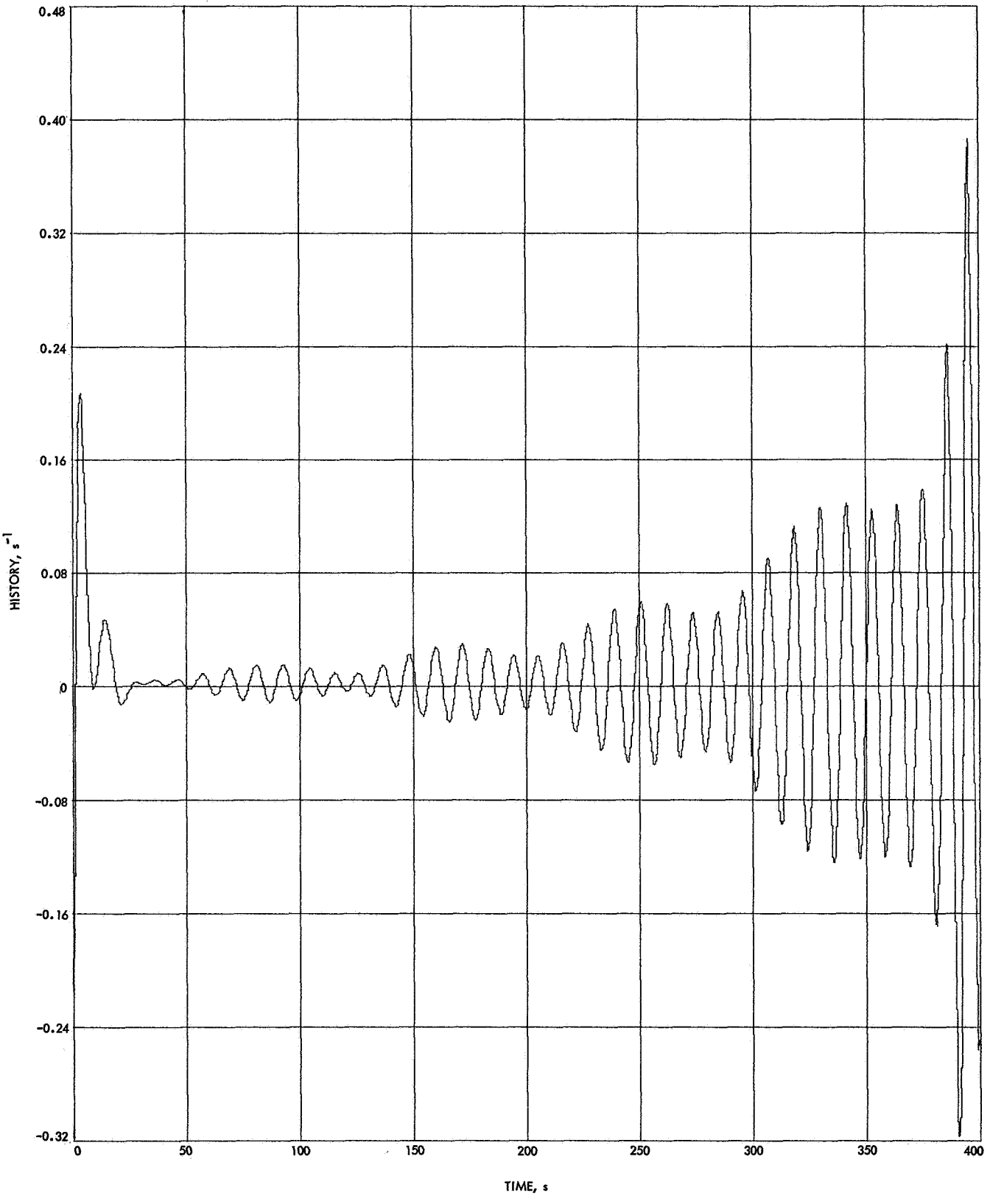

Fig. 21. Time history of inverse of determinant, case 2

Appendix A

Expression of $\mathbf{Q}(\omega)$

As mentioned in Section II-E, the thrusters occur in pairs and the matrix $\mathbf{Q}(\omega)$ is related to the resultant force and moment on the bus $\bar{\mathbf{F}}_X^o$ and to the forces on the appendages $\bar{\mathscr{F}}_m$ by Eq. (22). In the case of thrusters, because no local moment is applied on the bus but only concentrated forces, it is convenient to incorporate $\bar{\mathbf{F}}_X^o$ in the summation sign of the right side of Eq. (22) by letting the subscript m start from zero; i.e.,

$$\bar{\mathbf{F}}_X^o + \sum_{m=1}^{M} \mathbf{B}_m^T \mathbf{N}_m \bar{\mathscr{F}}_m = \sum_{m=0}^{M} \mathbf{B}_m^T \mathbf{N}_m \bar{\mathscr{F}}_m \tag{A-1}$$

In Eq. (A-1), $m = 0$ corresponds to the bus and $m \neq 0$ corresponds to an appendage. For the bus, $\mathbf{B}_0$ is a unit matrix and $\mathbf{N}_0$ reduces to a rigid-body-mode matrix:

$$[\mathbf{B}_0] = \begin{bmatrix} & 1 & \end{bmatrix} \tag{A-2}$$

$$\mathbf{N}_o = \boldsymbol{\phi}_R^T \tag{A-3}$$

Let it be assumed that there are six thrusters and that the ith thruster of intensity $\bar{F}_i$ is applied on the mth appendage at point M. Let $\boldsymbol{\alpha}_i$ be called the column of the direction cosines of thruster force $\bar{F}_i$ and, for convenience, $\boldsymbol{\alpha}_i$ will be taken with respect to the bus coordinates $OX_1X_2X_3$. The components of the ith thruster in the appendage coordinate are then

$$\bar{\mathscr{F}}_m = \mathbf{b}_m \boldsymbol{\alpha}_i \bar{F}_i \tag{A-4}$$

where $\mathbf{b}_m$ is the transformation matrix from the bus coordinates to the appendage coordinates.

There exists a $-i$th thruster that is equal and opposite to the corresponding ith thruster. Assume that this $-i$th thruster is applied on the nth appendage at point N:

$$\bar{\mathscr{F}}_n = -\mathbf{b}_n \boldsymbol{\alpha}_i \bar{F}_i \tag{A-5}$$

where $\mathbf{b}_n$ is the transformation matrix for the nth appendage. If one combines the three pairs of thrusters applied at points M, N, P, Q, S, and U, the right side of Eq. (A-1) becomes

$$\sum_{m=0}^{M} \mathbf{B}_m^T \mathbf{N}_m \bar{\mathscr{F}}_m = [\mathbf{B}_m^T \mathbf{N}_m^M \mathbf{b}_m \boldsymbol{\alpha}_1 - \mathbf{B}_n^T \mathbf{N}_n^N \mathbf{b}_n \boldsymbol{\alpha}_1] \bar{F}_1 + [\mathbf{B}_p^T \mathbf{N}_p^P \mathbf{b}_p \boldsymbol{\alpha}_2 - \mathbf{B}_q^T \mathbf{N}_q^Q \mathbf{b}_q \boldsymbol{\alpha}_2] \bar{F}_2 + [\mathbf{B}_s^T \mathbf{N}_s^S \mathbf{b}_s \boldsymbol{\alpha}_3 - \mathbf{B}_u^T \mathbf{N}_u^U \mathbf{b}_u \boldsymbol{\alpha}_3] \bar{F}_3 \tag{A-6}$$

where the superscript added to $\mathbf{N}_m$ indicates the location of the thrusters for the corresponding mode shapes.

Partitioning $\mathbf{Q}(\omega)$ yields

$$\mathbf{Q}(\omega) = [\mathbf{Q}_1 \,\vdots\, \mathbf{Q}_2 \,\vdots\, \mathbf{Q}_3] \tag{A-7}$$

where

$$\mathbf{Q}_1 = \mathbf{B}_m^T \mathbf{N}_m^N \mathbf{b}_m \boldsymbol{\alpha}_1 - \mathbf{B}_n^T \mathbf{N}_n^N \mathbf{b}_n \boldsymbol{\alpha}_1 \tag{A-8}$$

$$\mathbf{Q}_2 = \mathbf{B}_p^T \mathbf{N}_p^P \mathbf{b}_p \boldsymbol{\alpha}_2 - \mathbf{B}_q^T \mathbf{N}_q^Q \mathbf{b}_q \boldsymbol{\alpha}_2 \tag{A-9}$$

$$\mathbf{Q}_3 = \mathbf{B}_s^T \mathbf{N}_s^S \mathbf{b}_s \boldsymbol{\alpha}_3 - \mathbf{B}_u^T \mathbf{N}_u^U \mathbf{b}_u \boldsymbol{\alpha}_3 \tag{A-10}$$

If more than one thruster is applied on a given appendage (or the bus), the subscripts of Eq. (A-6) are repeated.

Finally, to construct the matrix $\mathbf{Q}(\omega)$, one needs:

(1) The direction cosines $\boldsymbol{\alpha}_i$ for each thruster pair.

(2) The location of each thruster.

(3) The mode shapes at each thruster location.

Appendix B

Numerical Computation of Fourier Transform

The Fourier transform pair relating a function $x(t)$ in the time domain to a complex function $X(f)$ in the frequency domain is

$$X(f) = \int_{-\infty}^{+\infty} x(t) \exp(-i2\pi ft)\, dt \tag{B-1}$$

$$x(t) = \int_{-\infty}^{+\infty} X(f) \exp(i2\pi ft)\, df \tag{B-2}$$

with the condition that

$$\int_{-\infty}^{+\infty} |x(t)|\, dt \tag{B-3}$$

is convergent.

In Eqs. (B-1) and (B-2), the frequency f is in Hz, and is related to ω by

$$\omega = 2\pi f \tag{B-4}$$

Equations (B-1) and (B-2) can be computed numerically using the fast Fourier transform algorithm (see Ref. 4), which permits a very rapid machine calculation.

It should first be noted that, because $x(t)$ is real, there must be

$$X(-f) = \overset{*}{X}(f) \tag{B-5}$$

where the asterisk means complex conjugate. This condition is satisfied for the system considered earlier. Consequently, Eq. (B-2) is replaced by

$$x(t) = 2\int_{0}^{\infty} X(f) \exp(i2\pi ft)\, df \tag{B-6}$$

The condition of Eq. (B-3) is satisfied if one considers a function $x(t)$ that tends towards zero for $t = \pm\infty$. For all practical purposes, the function $x(t)$ will have a non-zero value only for an interval of time T and will be zero outside this interval; i.e.,

$$\begin{aligned} &x(t) = 0 \text{ for } t < 0 \text{ and } t > T \\ &x(t) \neq 0 \text{ otherwise} \end{aligned} \tag{B-7}$$

Therefore, Eq. (B-1) is replaced by

$$X(f) = \int_{0}^{T} x(t) \exp(-i2\pi ft)\, dt \tag{B-8}$$

The fast Fourier transform algorithm requires that the function $x(t)$ be discretized into N discrete values where N is a power of 2:

$$N = 2^m \tag{B-9}$$

The discretized values of $x(t)$ are $x_0, x_1, \cdots, x_{N-1}$ at equally spaced times $t_0, t_1, \cdots, t_{N-1}$ in the interval $0,T$ (Fig. B-1); i.e.,

$$\begin{aligned} &t_j = j\,\Delta t \\ &j = 0, 1, 2, \cdots, N-1 \end{aligned} \tag{B-10}$$

where Δt is the time increment.

The corresponding frequency-domain values of $X(f)$ are $X_0, X_1, \cdots, X_{N-1}$ at the equally spaced frequencies $f_0, f_1, \cdots, f_{N-1}$ (Fig. B-2); i.e.,

$$\begin{aligned} &f_k = k\,\Delta f \\ &k = 0, 1, 2, \cdots, N-1 \end{aligned} \tag{B-11}$$

where Δf is the frequency increment; i.e.,

$$\Delta f = \frac{1}{T} = \frac{1}{N\Delta t} \tag{B-12}$$

The Fourier transform pair becomes

$$X_k = \Delta t \sum_{j=0}^{N-1} x_j W^{-jk} \tag{B-13}$$

and

$$x_j = 2\Delta f \sum_{k=0}^{N-1} X_k W^{jk} \tag{B-14}$$

where

$$W = \exp\left(\frac{2\pi i}{N}\right)$$

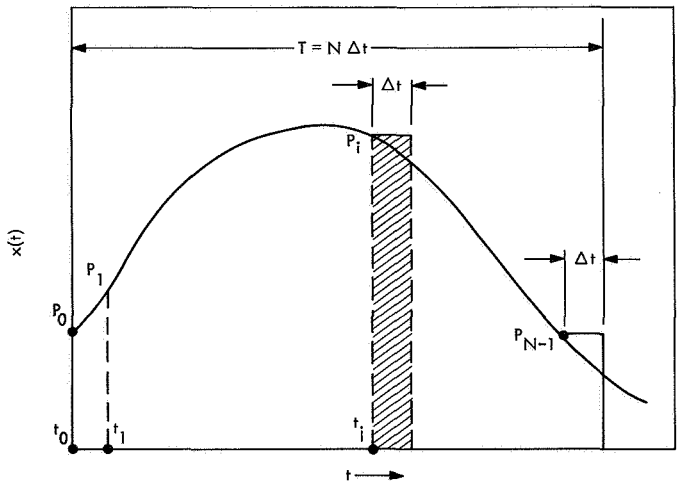

Fig. B-1. Discretization of x(t)

Then

$$x(t_j) = x_j$$

$$t_j = \frac{j}{N\Delta f} \tag{B-15}$$

and

$$X(f_k) = X_k$$

$$f_k = \frac{k}{N\Delta t} \tag{B-16}$$

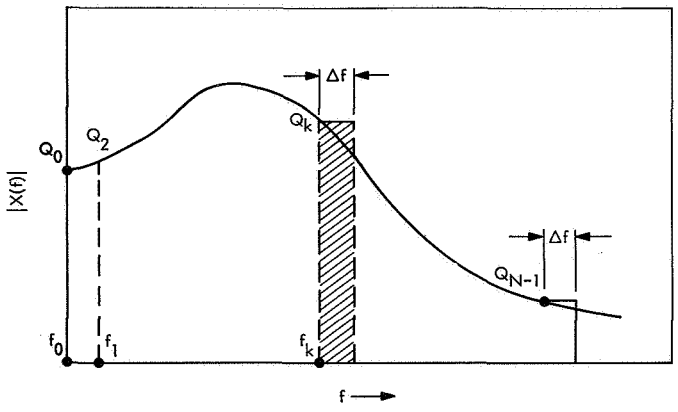

Fig. B-2. Discretization of X(f)

The summation of Eq. (B-13),

$$A(k) = \sum_{j=0}^{N-1} x_j W^{-jk} \tag{B-17}$$

is computed by the algorithm of Ref. 4 as a subroutine. The summation of Eq. (B-14) is identical to Eq. (B-17) except that $-j$ is changed to $+j$.

The value of N, taken herein from the actual program, was $N = 1024$.

Appendix C

Rigid-Body Mode for Appendage

The $3p \times 6$ rigid-body mode matrix ϕ_r corresponding to points $P_1, P_2, \cdots, P_p$ of an appendage is obtained by applying in turn, at the base A, a unit translation in the direction of each axis Ax_1, Ax_2, Ax_3 and a unit rotation about each of these axes. Because no local torque is applied at $P_1, P_2, \cdots, P_p$, only the translations of these points are considered. The expression of ϕ_r is

$$\phi_r = \left[\begin{array}{cccccc}
1 & 0 & 0 & 0 & y_3^1 & -y_2^1 \\
0 & 1 & 0 & -y_3^1 & 0 & y_1^1 \\
0 & 0 & 1 & y_2^1 & -y_1^1 & 0 \\
\hline
1 & 0 & 0 & 0 & y_3^2 & -y_2^2 \\
0 & 1 & 0 & -y_3^2 & 0 & y_1^2 \\
0 & 0 & 1 & y_2^2 & -y_1^2 & 0 \\
\hline
\multicolumn{6}{c}{\vdots} \\
\hline
1 & 0 & 0 & 0 & y_3^j & -y_2^j \\
0 & 1 & 0 & -y_3^j & 0 & y_1^j \\
0 & 0 & 1 & y_2^j & -y_1^j & 0 \\
\hline
\multicolumn{6}{c}{\vdots} \\
\hline
1 & 0 & 0 & 0 & y_3^p & -y_2^p \\
0 & 1 & 0 & -y_3^p & 0 & y_1^p \\
0 & 0 & 1 & y_2^p & -y_1^p & 0
\end{array}\right]$$

where y_1^j, y_2^j, y_3^j are the coordinates of points P_j $(j = 1, 2, \cdots, p)$ in appendage coordinates (see Fig. 2).

Nomenclature

$\mathbf{B}, \mathbf{B}_m$	geometric transformation matrix for mth appendage
$\mathbf{b}, \mathbf{b}_m$	submatrix of $\mathbf{B}$
$\mathbf{C}_{ee}$	generalized damping matrix of appendage
$\mathbf{D}, \mathbf{D}_m$	frequency-dependent matrix for mth appendage [Eq. (18)]
$\mathcal{F}_k$	components of forces on appendage
F_1, F_2, F_3	thruster forces
$\mathbf{F}$	column of thruster forces
$\mathbf{F}_X^O$	column of resultant forces and moment on bus
$\mathscr{F}^1, \mathscr{F}^2, \cdots, \mathscr{F}^p$	forces on appendages
$\mathscr{F}, \mathscr{F}_m$	column of components of forces applied on appendage
f, f_k	frequency, Hz
$\mathbf{f}_x^A$	column of reaction forces and moments at base of appendage
$\mathbf{f}_X^O$	column of resultant reaction forces and moments from appendage on bus

Nomenclature (contd)

$\mathbf{H}$ intermediate transfer function [Eq. (23)]

$\mathbf{H}_{XX}$ submatrix of $\mathbf{H}$

$\mathbf{H}_{X\theta}$ submatrix of $\mathbf{H}$

$\mathbf{H}_{\theta X}$ submatrix of $\mathbf{H}$

$\mathbf{H}_{\theta\theta}$ submatrix of $\mathbf{H}$

$\mathcal{H}_{\alpha\beta}$ terms of matrix $\mathcal{H}$

$\mathcal{H}$ system transfer-function matrix

$\mathcal{H}_1$ submatrix of $\mathcal{H}$

$\mathcal{H}_2$ submatrix of $\mathcal{H}$

$\mathcal{H}_3$ submatrix of $\mathcal{H}$

$h_{\alpha\beta}(t)$ terms of matrix $\mathbf{h}$

$\mathbf{h}$ response to unit-impulse matrix

$\mathbf{h}_1$ submatrix of $\mathbf{h}$

$\mathbf{h}_2$ submatrix of $\mathbf{h}$

$\mathbf{h}_3$ submatrix of $\mathbf{h}$

K_{jk} gain

$\overset{*}{K}_{jk}$ normalized gain

$\mathbf{K}_{ee}$ generalized stiffness matrix of appendage

$\mathbf{M}'$ mass matrix of bus

$\mathbf{M}_{ee}$ generalized mass matrix of appendage

$\mathbf{M}_{er}$ transpose of $\mathbf{M}_{re}$

$\mathbf{M}_{re}$ rigid elastic coupling matrix of appendage

$\mathbf{M}_{rr}$ rigid body mass matrix of appendage

$\mathcal{M}_{\alpha\beta}$ modulus of $\mathcal{H}_{\alpha\beta}$

m_j generalized masses

N number of discrete points

$\mathbf{N}, \mathbf{N}_m$ frequency-dependent matrix for mth appendage (Eq. 19)

$\mathbf{P}$ force torque transformation matrix

$\mathbf{Q}$ thruster force location matrix

$\mathbf{Q}_X$ submatrix of $\mathbf{Q}$

$\mathbf{Q}_\theta$ submatrix of $\mathbf{Q}$

$\mathbf{Q}_1$ submatrix of $\mathbf{Q}$

$\mathbf{Q}_2$ submatrix of $\mathbf{Q}$

$\mathbf{Q}_3$ submatrix of $\mathbf{Q}$

q_j generalized displacements

$\mathbf{q}$ column of generalized displacements of appendage

$R(\omega)$ inverse of determinant

$\mathbf{R}$ column of translations and rotations of bus

$\mathbf{r}$ column of translations and rotations of base of appendage

S_{jk} control loop

$\mathbf{S}$ control transfer-function matrix

$\mathbf{T}$ column of torques applied on structure

$\mathbf{T}_c$ column of control torques

$\mathbf{T}_d$ column of disturbance torques

t, t_j time

$X(f)$ Fourier transform of $x(t)$

X_1, X_2, X_3 coordinates of point A in bus coordinates

$\mathbf{X}$ translation of point O of bus

$x(t)$ arbitrary time function

Y^j_1, Y^j_2, Y^j_3 coordinates of P_j in appendage coordinates

$\mathbf{Y}$ structure transfer-function matrix

$\mathbf{Z}$ modal transfer function

α_l^{jk} control parameter

$\alpha_1, \alpha_2, \alpha_3$ direction cosine of thrusters

β_l^{jk} control parameter

γ_l^{jk} control parameter

$\Delta(\omega)$ determinant

δ_m^{jk} control parameter

$\delta(t)$ unit-impulse function

ϵ_m^{jk} control parameter

ξ_j modal damping

η_m^{jk} control parameter

$\theta_1(t)$ rotation of bus

$\theta_2(t)$ rotation of bus

$\theta_3(t)$ rotation of bus

$\boldsymbol{\theta}$ rotation of bus

ϕ_{jk} mode shapes at points of application of forces F_k

$\boldsymbol{\Phi}_e$ modal matrix for forces on appendage

Nomenclature (contd)

Φ_r rigid-body-mode matrix

$\psi_{\alpha\beta}$ phase angle of $\mathcal{H}_{\alpha\beta}$

ω circular frequency

ω_j natural frequencies

$\{\bar{}\}$ overbar means Fourier transform, Eq. (6)

References

1. Likins, P. W., *Dynamics and Control of Flexible Space Vehicles,* Technical Report 32-1329 (Revision 1). Jet Propulsion Laboratory, Pasadena, Calif., Jan. 15, 1970.
2. Hurty, W. C., and Rubinstein, M. F., *Dynamics of Structures.* Prentice-Hall, Inc., Englewood Cliffs, N.J., 1964.
3. Hurty, W. C., *Dynamic Analysis of Structural Systems by Component Mode Synthesis,* Technical Report 32-530. Jet Propulsion Laboratory, Pasadena, Calif., Jan. 15, 1964.
4. Cooley, J. W., and Tukey, T. W., "An Algorithm for the Machine Calculation of Complex Fourier Series," *Math. Comp.,* Vol. 19, pp. 297–301, 1965.

NASA — JPL — Coml., L.A., Calif.

N71-13063

TECHNICAL REPORT STANDARD TITLE PAGE

1. Report No. 32-1478	2. Government Accession No.	3. Recipient's Catalog No.
4. Title and Subtitle A FREQUENCY DOMAIN SOLUTION FOR THE LINEAR ATTITUDE-CONTROL PROBLEM OF SPACECRAFT WITH FLEXIBLE APPENDAGES		5. Report Date November 15, 1970 6. Performing Organization Code
7. Author(s) M. R. Trubert		8. Performing Organization Report No.
9. Performing Organization Name and Address JET PROPULSION LABORATORY California Institute of Technology 4800 Oak Grove Drive Pasadena, California 91103		10. Work Unit No. 11. Contract or Grant No. NAS 7-100 13. Type of Report and Period Covered Technical Report
12. Sponsoring Agency Name and Address NATIONAL AERONAUTICS AND SPACE ADMINISTRATION Washington, D.C. 20546		14. Sponsoring Agency Code

15. Supplementary Notes

16. Abstract

The three-dimensional linear interaction problem between attitude control of spacecraft and the flexibility of spacecraft is solved in the frequency domain by using the concept of Fourier transform. The transfer-function matrix of the system formed by the linear structure and the linear control circuit is determined from the modal characteristics of the structure, using the modal combination concept and the electrical characteristics of the control loop. A large number of elastic modes can be used for the structure. Time histories are obtained by inverse Fourier transformation. The three angles of the attitude of the spacecraft with respect to an inertial frame of reference are computed for any disturbance torques applied about the three axes of the spacecraft. A stability study is made by direct inspection of the responses to unit impulse for the three attitude angles or, alternatively, by the display of a determinant. A computer program has been written to compute all of the necessary transfer functions, and the last Fourier transform algorithm has been used to compute Fourier transforms. The program is used on a teletype terminal.

17. Key Words (Selected by Author(s))	18. Distribution Statement
Control and Guidance Interplanetary Spacecraft, Advanced Structural Engineering	Unclassified -- Unlimited

19. Security Classif. (of this report)	20. Security Classif. (of this page)	21. No. of Pages	22. Price
Unclassified	Unclassified	30	

HOW TO FILL OUT THE TECHNICAL REPORT STANDARD TITLE PAGE

Make items 1, 4, 5, 9, 12, and 13 agree with the corresponding information on the report cover. Use all capital letters for title (item 4). Leave items 2, 6, and 14 blank. Complete the remaining items as follows:

3. Recipient's Catalog No. Reserved for use by report recipients.

7. Author(s). Include corresponding information from the report cover. In addition, list the affiliation of an author if it differs from that of the performing organization.

8. Performing Organization Report No. Insert if performing organization wishes to assign this number.

10. Work Unit No. Use the agency-wide code (for example, 923-50-10-06-72), which uniquely identifies the work unit under which the work was authorized. Non-NASA performing organizations will leave this blank.

11. Insert the number of the contract or grant under which the report was prepared.

15. Supplementary Notes. Enter information not included elsewhere but useful, such as: Prepared in cooperation with... Translation of (or by)... Presented at conference of... To be published in...

16. Abstract. Include a brief (not to exceed 200 words) factual summary of the most significant information contained in the report. If possible, the abstract of a classified report should be unclassified. If the report contains a significant bibliography or literature survey, mention it here.

17. Key Words. Insert terms or short phrases selected by the author that identify the principal subjects covered in the report, and that are sufficiently specific and precise to be used for cataloging.

18. Distribution Statement. Enter one of the authorized statements used to denote releasability to the public or a limitation on dissemination for reasons other than security of defense information. Authorized statements are "Unclassified—Unlimited," "U. S. Government and Contractors only," "U. S. Government Agencies only," and "NASA and NASA Contractors only."

19. Security Classification (of report). NOTE: Reports carrying a security classification will require additional markings giving security and downgrading information as specified by the Security Requirements Checklist and the DoD Industrial Security Manual (DoD 5220.22-M).

20. Security Classification (of this page). NOTE: Because this page may be used in preparing announcements, bibliographies, and data banks, it should be unclassified if possible. If a classification is required, indicate separately the classification of the title and the abstract by following these items with either "(U)" for unclassified, or "(C)" or "(S)" as applicable for classified items.

21. No. of Pages. Insert the number of pages.

22. Price. Insert the price set by the Clearinghouse for Federal Scientific and Technical Information or the Government Printing Office, if known.